NTNU

Norwegian University of
Science and Technology

Determination of Fe(II) and Fe(III) in *Synechococcus* sp. PCC 7002 culture

Maria Villegas

Environmental Toxicology and Chemistry
Submission date: May 2018
Supervisor: Murat Van Ardelan, IKJ

Norwegian University of Science and Technology
Department of Chemistry

Acknowledgments

I would like to thank my supervisor Murat Ardelan for introducing me into the field of marine chemistry and for his enthusiasm that is always motivating. I would also like to thank Annie Vera for all of her hard-work in this project and for being a great mentor. Also, Ayten Pehlivan for her collaboration on the biological measurements and her positive attitude. Anne Vogel for providing us with the *Synechoccocus* babies and always having a wealth of knowledge. Nicolas Sanchez for his help and encouragement. I also want to thank Syverin for running the numerous ICP-MS samples.

To my friends in Trondheim for making everything better. My family for their love and humorous outlook in life that is contagious. To my Digernes family for receiving me with open arms and helping me adjust in Norway in the best possible way. To Einar, whom I owe immense gratitude for his endless support.

Para mi mamá, quien ha sido un gran ejemplo y me ha enseñado lo que es trabajar duro.

Abstract

Iron speciation analysis is important to enhance our understanding of iron's role in limiting phytoplankton productivity in the ocean. In this study, two different particulate Fe species, crystalline particle goethite (FeO(OH)) and $FeCl_3$ are used in cyanobacteria *Synechococcus* sp. PCC 7002 culture to test for a potential reduction mechanism. It has been suggested that some photosynthetic prokaryotic strains may employ cell surface Fe(III) reduction mechanism for iron oxides to produce bioavailable Fe(II) [53, 51]. Notably, iron is often present in seawater in the form of insoluble iron oxides to which its bioavailability is poorly understood. To demonstrate biogenic Fe(III) reduction, Fe(II) and Fe(III) (TFe and dFe) are determined using *in line* Flow injection analysis with chemiluminescence detection and ICP-MS with seaFAST respectively. Our results show that Fe(II) production is detected in a culture grown with FeO(OH) (0.19±0.19nM n=9) and a culture with $FeCl_3$ (0.30±0.22nM, n=10). In addition, Fe(II) is detected for abiotic control samples in FeO(OH) (0.06±0.07nM, n=9) and $FeCl_3$ (0.04±0.22nM, n=10). Thus, Fe(III) reduction may be photochemically produced under photosynthetically active radiation (PAR). In addition, dFe concentration increases in culture with goethite day 1 (7.69±0.52nM, n=3) and day 22 (35.49±3.69nM, n=3). However, culture growing with $FeCl_3$ shows decrease in dFe concentration from day 8 samples (40.53±2.23nM dFe, n=3) and day 23 (3.26±1.95nM dFe, n=3). This may infer different reduction rates between amorphous iron oxides and crystalline forms of iron [3]. This work implicates a biologically mediated reduction of particulate Fe(III) due to higher Fe(II) and dFe concentrations for *Synechococcus* sp. PCC 7002 with $FeCl_3$ and FeO(OH) relative to abiotic control.

CONTENTS

Acronyms

chl-a Chlorophyll a

EDTA ethylenediaminetetraacetic acid

FIA-CL Flow injection analysis chemiluminescence

HDPE High density polyethylene

HNLC High nutrient low chlorophyll

HPLC high performance liquid chromatography

HR-ICP-MS High resolution inductively coupled plasma mass spectrometry

LED light emitting diode

LDPE low density polyethylene

LoD limit of detection

OD Optical density at 730nm wavelength

PAR photosynthetically active radiation

PFA per-fluoroalkoxy copolymer material

PMT Photon multiplier detector

sp. PCC 7002 single species pasteur culture collection

SOW synthetic ocean water

TFe total iron, also referred to as total dissolvable iron (TDFe)

UHP Ultra- high purity

Chapter 1

INTRODUCTION

Iron is an essential element required by all aerobic organisms for vital processes such as photosynthesis, respiration, nitrogen fixation and many other key processes [100, 71]. However, in many areas of the open ocean iron is generally unavailable with dissolved concentrations at sub-nanomolar levels [116, 112]. The marine chemistry of iron is complex due to thermodynamic factors that cause low iron solubility in oxic conditions [28]. As a result, it is reported that marine phytoplankton are limited by iron supply in 30-40% of the world's oceans [18, 115, 70]. Marine phytoplankton are a critical group of organisms provided that they are responsible for a large amount of absorption of the earth's atmospheric carbon dioxide [30].

Iron limitation in the ocean has not always been prominent knowledge. Areas in the ocean known as high nutrient low chlorophyll (HNLC) zones contain sufficient nutrients but relatively low primary productivity [75, 16]. HNLC zones contain significantly high levels of nitrate, phosphate and silicate throughout the year but do not produce phytoplankton biomass blooms in the spring [111]. Oceanographer John Martin hypothesized that iron is limited in HNLC zones of the ocean [63]. However, many early studies of iron in the ocean lacked proper techniques to measure iron accurately. This is due to the ubiquitous nature of iron in the atmosphere and in our laboratory equipment present as dust which can contaminate samples. The development of a clean room driven primarily by scientist Clair

Patterson greatly reduced contamination during elemental analysis [79, 80]. John Martin and other scientists implemented these clean techniques to study oceanic iron concentrations [62]. Trace metal clean techniques eventually revealed that iron is the limiting factor in HNLC regions of the ocean [6, 21].

Iron speciation is a key component in revealing iron availability to marine organisms. In the ocean iron occurs in two main redox states, one as dissolved Fe (II) which rapidly oxidizes to form insoluble Fe (III) [32, 72, 129]. In addition, iron often forms inorganic and organic complexes [35, 65], colloids [134] and particulate fractions [33] of which formations have a strong influence on the fate of iron in the ocean. Fe(III) in the ocean has extremely low solubility and rapidly hydrolyzes which results in the formation of particulate Fe(III) oxides or hydroxide phases. As a result, Fe(III) in the ocean is predominantly in particulate iron oxyhydroxide form [52, 58]. It is also reported that more than 99% of dissolved iron in seawater is bound to organic material [35]. The bioavailability of most of these complexes are not fully understood, therefore elucidating the importance of speciation studies.

However, iron analysis in seawater matrices has many challenges. Analytical steps should prevent altering iron speciation and the introduction of contamination. Specifically, Fe(III) analysis in seawater can have interferences due to high salt concentrations and may require pre-concentration to determine sub-nanomolar iron concentrations. The pre-concentration process is subject to many analytical procedures at risk for iron contamination. Moreover, Fe(II) analysis has unique analytical challenges due to its short-life and highly reactive nature. Factors like pH, light, temperature, dissolved oxygen, natural organic material (NOM) and reactive oxygen species (ROS) affect Fe(II) oxidation [76]. For instance, in oxic conditions Fe(II) easily forms Fe (III) [58, 98]. Fe(II) also oxidizes at a faster rate as tempera-

ture increases [24]. Hence, few studies report Fe(II) production analysis on marine phytoplankton [56] [86]. Two leading methods for Fe(II) analysis in water are flow injection analysis with chemiluminescence FIA-CL [28, 133] and spectrophotometric methods [39, 15].

Many iron studies aim to understand interactions between photosynthetic organisms and iron. Cyanobacteria, known as the oldest photosynthetic prokaryotes, evolved about 3.5 billion years ago and account for 25% of global ocean net primary productivity [121]. In addition, cyanobacteria have higher iron requirements than their eukaryotic competitors [69], which makes them suitable for iron studies. Despite the scarcity of directly bioavailable iron in the ocean, marine photosynthetic organisms have developed survival methods to obtain iron from various sources [99] [43] [53]. Some cyanobacteria strains such as *Synechocystis* sp. PCC 6803 show a reduction method using a protein called pili with capabilities for Fe(III) reduction to Fe(II) through electron donation to extracellular electron acceptors [53] [36]. The reduction in *Synechocystis* sp. PCC 6803 occurs before transport through the plasma membrane [51]. Some researchers suggest that a similar pili mechanism may be present in *Synechococcus sp.* PCC 7002 [123]. Other work shows the production of organic complexes that bind iron in response to iron stress in *Synechococcus sp.* PCC 7002 [131, 37].

This work studies Fe(III) reduction through determination of Fe(II), total and dissolved iron (TFe and dFe) to follow iron speciation changes in *Synechococcus* sp. PCC 7002 culture using FIA-CL and ICP-MS with seaFAST pre-concentration respectively. Two different forms of Fe(III) salts, $FeCl_3$ and FeO(OH) are use to give insight into changes in iron uptake by *Synechococcus* sp. PCC 7002.

1.1 Hypothesis

Synechococcus sp. PCC 7002 may be able to reduce particulate Fe(III) to soluble and bioavailable Fe(II) by electron flux mechanism. To follow this biogenic reduction of iron the determination of dissolved Fe(II) and Fe(III) in the culture is essential. We expect that different species of particulate Fe(III) may have different response for this biogenic surface reduction mechanism, such as amorphous iron oxides and crystalline iron oxy hydroxide (FeO(OH)) may have different reduction and bioavailable potential.

1.2 Objectives

Main objectives:

1. To determine soluble Fe(II) and Fe(III) concentration using in line FIA-CL and ICP-MS with seaFAST respectively to follow Fe transformation in *Synechococcus* sp. PCC 7002.

2. To optimize method sensitivity for quantification of iron (II) by FIA-CL method in cyanobacteria *Synechococcus* sp. PCC 7002 culture.

Sub-goals:

- Incubation of cyanobacteria culture under constant temperature and light in synthetic ocean water with nutrients.

- To improve seaFAST pre-concentration efficiency.

- To implement clean techniques for trace level iron studies in laboratory and field studies.

1.3 Collaborations

This is a collaboration thesis with master student Ayten Pehlivan, who focuses on biological studies to unveil complementary information about *Synechococcus* sp. PCC 7002 during iron acquisition.

Chapter 2

THEORETICAL BACKGROUND

2.1 Iron fractions

Iron species are crucial to define and determine in order to understand the processes that govern iron biogeochemistry and cycling in the ocean. Speciation refers to the physical and chemical forms of an element such as oxidation states, complexes, ion pairs, colloidal and particle forms. Specifically, iron can be divided into multiple fractions such as particulate (PFe), dissolved (dFe), soluble (sFe) and colloidal (cFe), which can be operationally defined by particle size filtration [124]. Figure 2.1 shows the size scale and examples of these iron fractions. However, these size definitions are strictly operational and consequently not fully descriptive of inorganic, organic or reactivity states as demonstrated by overlap and dotted lines in Fig. 2.1. As mentioned in the introduction, iron in the ocean can exist in two oxidation states, Fe(II) and Fe(III). These iron oxidation states are predominantly present in the ocean with inorganic and organic complexes. The smallest fraction of the dissolved iron pool known as soluble Fe, passes through $\leq 0.02\mu$m pore size filter [134] and includes organic and inorganic fractions of iron. The inorganic sFe describes free inorganic iron species such as $FeCl^{-}$ and Fe^{2+}. Fractions of inorganic iron such as $FeCl_3$ rapidly form amorphous iron oxide complexes (Fe(OH)x) [74]. The organic portion of sFe includes Fe complexes with organic lig-

ands. Organic-iron complexes are widely studied today as they form >99% of the dissolved iron pool [35] although their bioavailability is yet not fully understood. It has been widely shown that Fe-binding ligands are released by microorganisms which increases iron solubility [90, 42, 91, 120].

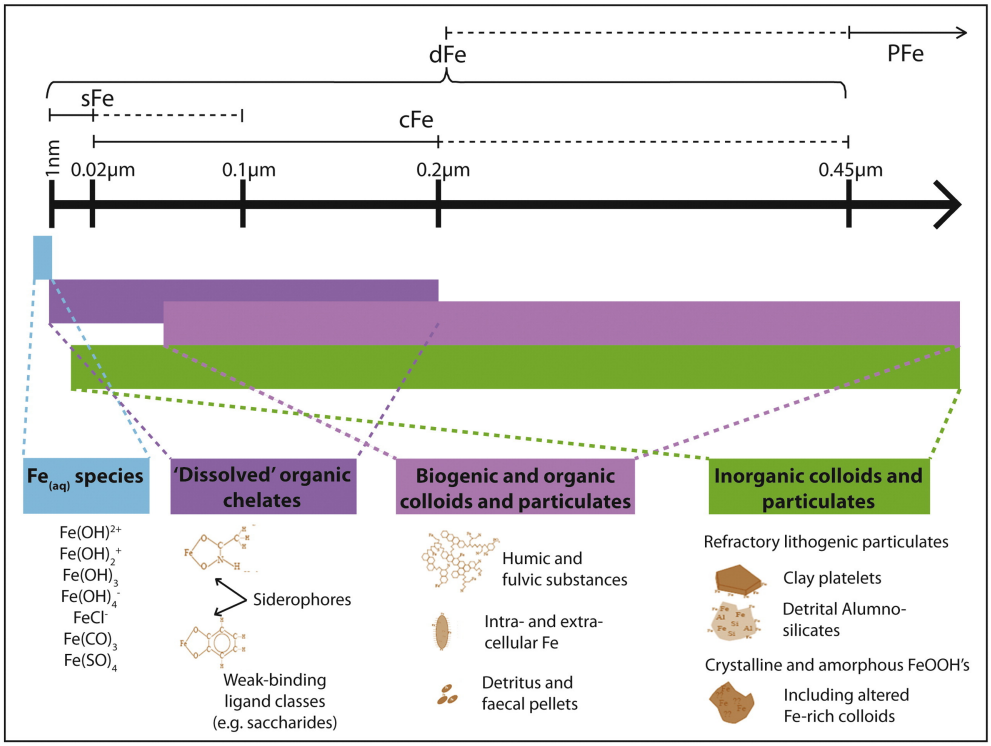

Figure 2.1: Chemical forms of iron with operationally defined iron size classes. Source: [124] originally adapted from [119]

In short, dissolved iron is defined operationally by the fraction that goes through filtration using pore size $\leq 0.2\mu$m or 0.45μm which includes colloidal and soluble iron (Fig. 2.1). Colloidal iron concentrations can be obtained from the concentration difference between dissolved and soluble iron [134]. Therefore, colloidal iron is a fraction in the dissolved iron pool that is between 0.02-0.45 μm pore size. The organic composition of colloidal iron includes some larger and weaker iron

siderophore complexes relative to sFe such as humic substances, smaller biogenic material like viruses and detrius material. Inorganic colloidal material includes lithogenic particulates and crystalline and amorphous iron oxides and hydroxides that are cycling between particulate iron pool. The colloidal portion of the dissolved iron pool is not available to all marine organisms and is poorly understood. Although the bioavailability of colloidal iron shows to be dependent on particle size and origin of colloid material [126, 26]. In the ocean, colloidal form of iron comprises 90% of the dissolved iron fraction in coastal waters and less than 10% in pelagic region [132, 134, 8].

Additionally, particulate iron is the fraction collected that does not go through a 0.2μm or 0.45μm pore size filter. Particulate iron occurs either as inorganic or adsorbed to or complexed with organic particles. The inorganic iron forms include refractory authigenic and large lithogenic iron. Lithogenic iron is present as oxyhydroxides, silicates and aluminosilicates that either sinks into the deep ocean [26] or converts to the biogenic particulate iron pool [33]. A large portion of inorganic particulate (and colloidal) material in the ocean exists as hydroxides or oxides [52]. In oceanic conditions inorganic Fe(III) readily hydrolyses forming oxyhydroxides that over time form more refractory iron oxides [20, 52]. As a result Fe(III) is predominantly in iron (hydr)oxide complexes [68, 52]. A list of common iron oxides and hydroxides is shown in Figure 2.2. Solubility of these compounds varies depending on pH, temperature and salinity [57].

In seawater pH 8, particles such as oxides or hydroxides bind positively charged iron thus forming particles that can be scavenged from water column by sinking to depth. Therefore, iron that binds to hydroxides or oxides is less bioavailable due to their adsorption to sinking particles [58]. In addition, particle Fe(III) hydroxides

Oxide–hydroxides and hydroxides	*Oxides*
Goethite α-FeOOH	Hematite α-Fe_2O_3
Lepidocrocite γ-FeOOH	Magnetite Fe_3O_4 ($Fe^{II}Fe^{III}_2O_4$)
Akaganéite β-FeOOH	Maghemite γ-Fe_2O_3
Schwertmannite $Fe_{16}O_{16}(OH)_y(SO_4)_z \cdot n\ H_2O$	β-Fe_2O_3
δ-FeOOH	ε-Fe_2O_3
Feroxyhyte δ′-FeOOH	Wüstite FeO
High pressure FeOOH	
Ferrihydrite $Fe_5HO_8 \cdot 4\ H_2O$	
Bernalite $Fe(OH)_3$	
$Fe(OH)_2$	
Green Rusts $Fe^{III}_xFe^{II}_y(OH)_{3x+2y-z}(A^-)_z$; $A^- = Cl^-$; $^1/_2\ SO_4^{2-}$	

Figure 2.2: Different types of iron oxides and oxide-hydroxides. Source: [23]

such as goethite (FeO(OH)) is present in crystalline form which has extremely low solubility. While other forms of particulate iron goes through recycling and grazing as it is adsorbed to biogenic and detrial material which includes organisms such as phytoplankton and bacteria [118]. Finally, Total iron (TFe) is operationally defined by the total fraction detected after acidification without any filtration [122].

2.2 Iron cycling in the ocean

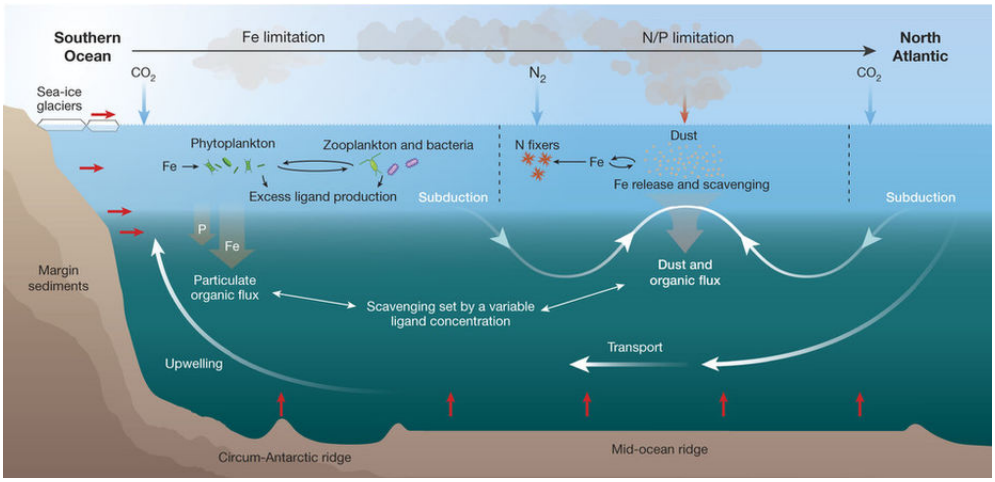

Figure 2.3: Major processes in the ocean iron cycle. Source: [115]

Iron cycling is important for the distribution of primary productivity in the ocean. Iron cycling in the ocean is driven by sources, sinks and iron speciation. Sources of iron include atmospheric dust, river input, melting of sea ice, upwelling, sediments and hydrothermal vents [85]. One major source of iron in the ocean is atmospheric dust as shown in Figure 2.4 where atmospheric dissolved iron estimations accounts for a relatively large annual global flux ($1.8-2.1 \times 10^{12}$g) in the ocean [22, 114, 133]. Although a large fraction of atmospherical iron is highly refractory [1, 89]. In addition, water mixing through upwelling is an important iron supply in areas where atmospheric deposition of iron is scarce[41]. Aerosol iron is introduced and acquired by biological organisms in the photic zone such as diazotrophs[89] and iron cycles between biological communities (i.e. diatom, flagellate, picoprokaryote, picoeukaryote, heterotrophic bacterium) [120] as shown in Figure 2.3 [115]. Iron cycles by being mineralized through the digestive tracts of marine microorganisms

and released into the photic zone [99]. Organic ligands retain iron in solution and contribute to the horizontal movement of the dissolved iron pool in the ocean[2, 19, 14]. Although not all dissolved iron may be available to all organisms.

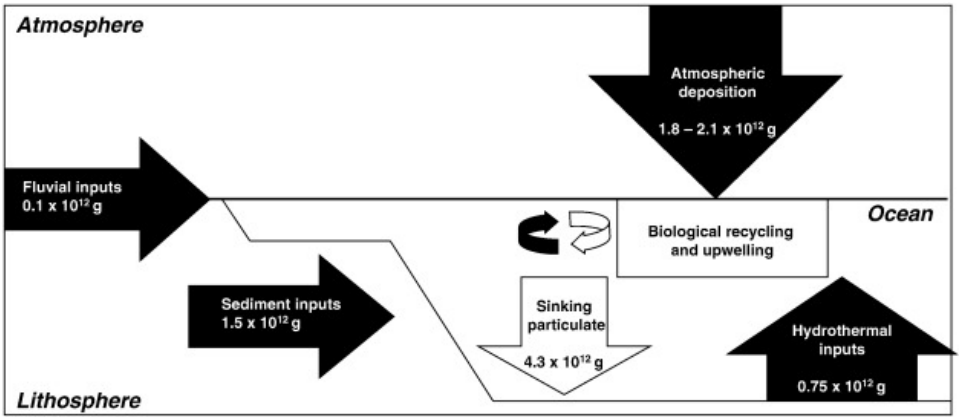

Figure 2.4: Approximations for annual global fluxes of dissolved iron to the ocean. Source: [133] with original values obained from [136, 109, 17]

A major sink for iron is sinking particulate including scavenging[120]. This can be seen in Figure 2.4 where a relatively large annual amount of particulate iron sinks (4.3×10^{12}g)[117]. Dissolved iron that enters the ocean through fluvial inputs (0.1×10^{12}g) is often trapped in coastal areas by forming inorganic and organic complexes [133]. Overall, retention of iron supply from external sources occurs by abiotic and biotic mechanisms in which is essential for internal iron cycling.

2.3 Marine Phytoplankton

Marine phytoplankton compose more than 45% of the photosynthetic net primary production on earth [106]. The term marine phytoplankton represents a large

diverse group of prokaryotes and eukaryotes that obtain energy through photosynthesis. This photosynthesis originated with the process known as endosymbiosis. Bacteria and Eukarya are the two main domains in marine plankton. Diatoms, dinoflagellates and haptophytes dominate the phytoplankton groups of species in marine phytoplankton[120].

Bacteria have played a vital role in the evolution of phytoplankton. Cyanobacteria have been credited as the first organisms oxygenating the earth through photosynthesis [101, 93]. As a result this lead to the development of aerobic organisms [49]. Cyanobacteria are the most widely distributed and diverse group of photosynthetic bacteria. This is due to their simple nutritional requirements such as light, carbon source, inorganic salts, sulfur and phosphorus. Nevertheless, these organisms require relatively high amounts of iron due to their photosynthetic and cytochrome demands [46, 9]. The greatest requirement for iron in phytoplankton is in the photosynthetic systems. Photosystem I and II (PSI and PSII) require 12 and 2-3 Fe atoms respectively [84]. In addition, cytochrome c and b6f use iron for photosynthetic and respiratory electron transfer chains. Iron is also part of the nitrate assimilation and nitrogen fixing enzymes. In addition, *Synechococcus* sp. PCC 7002 is a unicellular photosynthetic cyanobacterium which can grow among a high range of NaCl conditions [60]. The doubling time can be 2.6 hours under optimal conditions which include 38°C, 1% v/v CO_2 in air and light conditions of 250μmol photons $m^{-2}s^{-1}$.

2.3.1 Iron uptake

Two major but not exclusive mechanisms for iron acquisition in cyanobacteria are reported. Firstly, siderophore production by cyanobacteria under iron limiting conditions [130, 43, 95]. This involves the synthesis and secretion of chelators that bind Fe^{3+} and complex is transported into cell where iron is obtained [53]. However, many cyanobacteria lack genes for the production of siderophores [29, 36]. In addition, cyanobacteria show the uptake of siderophores produced by other nearby organisms [45]. Secondly, some cyanobacteria strains such as *Synechocystis sp.* PCC 6803 show a pilA method with capabilities for Fe(III) reduction [53]. Pili are extracellular appendages protein fibers that have many functions like motility [10], DNA uptake [11] and with the use of electrically conductive surface structures that facilitate external electron acceptors [53]. Finally, other mechanisms involve citrate Fe^{3+} chelating properties [43] and protein synthesis methods for iron acquisition [54, 34]

2.4 Flow injection analysis

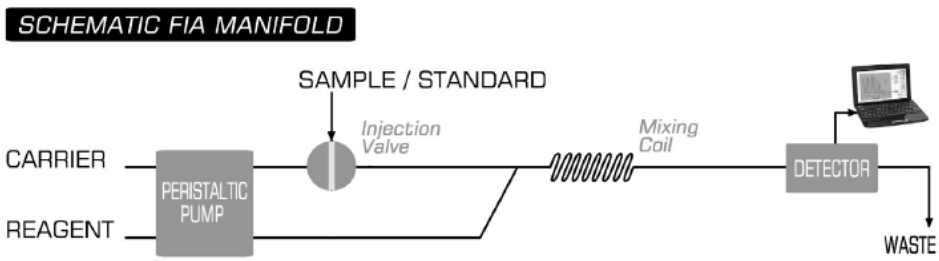

Figure 2.5: Schematic diagram of flow injection analysis. Source: [132]

Flow injection analysis (FIA) was first introduced in 1975 [92]. Today FIA is the most widely used method for iron analysis due to its ability to distinguish between the two redox species Fe(II) and Fe(III) and low sample consumption. In addition, FIA has high sensitivity, rapid detection and portability and hence a possibility for shipboard deployment.

2.4.1 Method overview

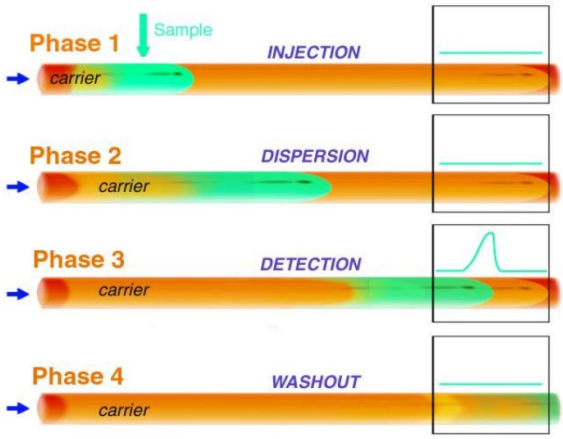

Figure 2.6: Stages of flow injection analysis. Source: [104]

Flow injection analysis is based on the flow of a carrier through a moving sample which can be detected by its reaction with a reagent.The sample enters after injection from valve which creates flow stream between sample and carrier as shown in phase 1 on Figure 2.6. The sample is dispersed by the carrier during phase 2 and sample mixes with reagent in phase 3 in the mixing coil followed by detection as shown in Figure 2.5. Once sample enters detection phase the carrier activates washout step to prepare for next sample. In some set-ups the reagent can serve

as the carrier and reagent thus requiring fewer channels. In other cases analytes require several reactions thus more channels and carriers. The basic components of a flow injection system are reagent, carrier, valve, pump, reaction coil and flow cell detection system as shown in Figure 2.5.

2.4.2 Chemical reaction

Flow injection luminol based method uses luminol as the reagent and chemiluminescence as the detection method. Luminol (5-amino-2,3-dihydro-1,4-phthalazinedione) is a compound that emits light when oxidized. The first step of the reaction as shown in Figure 2.7 is the oxidation of luminol to luminol radical intermediate. This first step is facilitated by the reaction of superoxide with carbon dioxide, from potassium carbonate, to produce peroxycarbonate radical as shown in this equation.

$$CO_2 + {O_2}^- \longrightarrow {CO_4}^- \tag{2.1}$$

Superoxide radical is formed by the oxidation of iron II by oxygen as seen in the reaction below.

$$Fe^{2+} + O_2 \longrightarrow Fe^{3+} + {O_2}^- \tag{2.2}$$

Superoxide formed by iron (II) oxidation then facilitates the formation of aminophtalate and nitrogen. Aminophtalate ion emits light that can be detected by chemi-

luminescence [87, 24]. The optimal reaction conditions for the oxidation of iron (II) and thereby production of superoxide are at pH 10.1.

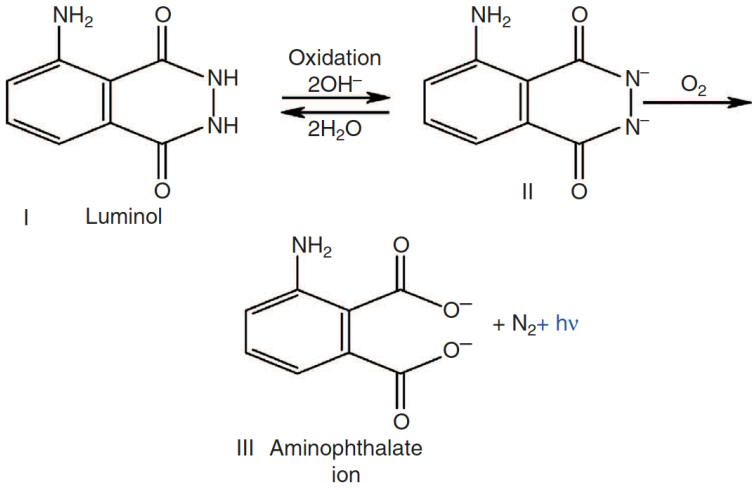

Figure 2.7: Chemiluminescence reaction of luminol (I) where superoxide intermediate (not shown) is formed by oxidation of iron(II) resulting in aminophthalate iron(III) which is a light-emitting specie. Source: [44]

2.4.3 Detection

Once signal reaches detector, a graph of time versus detector response is produced. To calculate iron (II) concentrations of unknown sample, a calibration run is employed daily with known Fe(II) concentration standards prepared immediately before analysis. A calibration curve is plotted for response area versus concentration of standards. Concentration of iron (II) in unknown samples is determined from slope and intercept of regression line in calibration graph. Alternatively, peak height can be used for determination of concentrations. It is reported that results based on peak height are around 4-5% lower than results based on peak area [32]. This is likely due to asymmetry of peaks [127] which affects area. Overall esti-

mated uncertainties are higher for peak height due to larger uncertainty related to sensitivity coefficient for peak height compared to peak area [32]. Therefore, peak area is the preferred method for quantification on FIA-CL.

2.4.4 Fe(II) oxidation

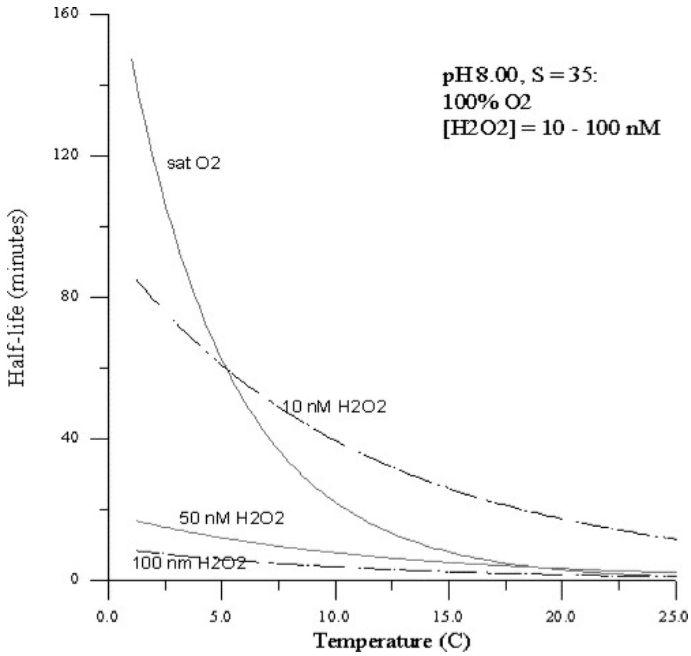

Figure 2.8: Half-life of iron as a function of temperature and oxidant concentrations of oxygen and H_2O_2. Source: [24]

Oxidation of Fe(II) occurs more rapidly as a function of temperature in the presence of saturated oxygen levels as shown in Figure 2.8 [24]. The half-life of iron is higher at colder temperatures due to slower kinetics for the oxidation step [48]. Hydrogen peroxide concentrations also have an effect on iron (II) oxidation rates due its ability to oxidize Fe(II) [66, 96]. In the oceans hydrogen peroxide can be produced

by photochemical processes [77] or the oxidation of Fe(II) as shown in Haber-Weiss mechanism in equation 2.3 [88]. Hydrogen peroxide also functions as an oxidant of Fe(II) as shown in (Eq. 2.4 and 2.5).

$$\mathrm{Fe(II)} + \mathrm{O_2}^- \longrightarrow \mathrm{Fe(III)} + \mathrm{H_2O_2} \tag{2.3}$$

$$\mathrm{Fe(II)} + \mathrm{H_2O_2} \longrightarrow \mathrm{Fe(III)} + \mathrm{OH^{\cdot}} + \mathrm{OH^-} \tag{2.4}$$

$$\mathrm{Fe(II)} + \mathrm{OH^{\cdot}} \longrightarrow \mathrm{Fe(III)} + \mathrm{OH^-} \tag{2.5}$$

The oxidation rate of Fe(II) (Eq. 2.6) (originally presented by [67]) is described by k_{app} which is the sum of the oxidation rates of individual Fe(II) species. $[O_2]$ and [Fe(II)] represents total oxygen and Fe(II) concentration and α_1 represents the fraction of each Fe(II) species in a solution.

$$-\frac{\mathrm{d}\{\mathrm{Fe(II)}\}}{\mathrm{d}t} = [\mathrm{O_2}]\{\mathrm{Fe(II)}\}k_{\mathrm{app}}$$
$$k_{\mathrm{app}} = 4(k_1\alpha_{\mathrm{Fe^{2+}}} + k_2\alpha_{\mathrm{FeOH^+}} + k_3\alpha_{\mathrm{Fe(OH)_2{}^0}} + \ldots k_n\alpha_n) \tag{2.6}$$

2.4.5 Alternative Fe(II) methods

Other methods for Fe(II) detection include FIA with spectrophotometry as a detector and ferrozine as a ligand [110, 47]. Ferrozine is a selective ligand for Fe(II) that is added to a sample which then passes through a C_{18} resin for pre-concentration of Fe(II) ions. Sample passes through a chelating resin to form complex with ferrozine then ferrozine-Fe(II) complex is eluted with methanol and detected with a spectrophotometer. A similar method using liquid chromatography is also reported for freshwater determination of Fe(II) [137].

2.5 SeaFAST

SeaFAST is a pre-concentration instrument used for seawater by allowing seawater matrix ions such as $Na^+Cl^-Ca^{2+}$ etc. to waste while retaining a variety of transition metals and rare-earth elements in the column. Specifically, concentration can be achieved for trace metals (Mn, Fe, Ni, Cu, Zn), transition metals (Ti, Nb, V, Mo, W, Zr), labile cobalt, and rare-earth metals [38]. The acidified sample (pH $\leq$ 2) is introduced by an autosampler probe and fills a 10mL PTFE sample loop. In addition, the seaFAST system contains a cleaning column for the removal of trace metals in ammonium acetate buffer and carrier MilliQ water. The ammonium acetate buffer mixes with the sample and water mixture before entering the chelation column. Sample mixture is then pushed into the chelation column where elements are chelated and the matrix is removed. The chelation column resin contains iminodiacetic and ethylenediaminetriacetic acid functional groups that chelates metals mentioned above [107]. The pH of the chelation column is maintained at pH 6

by a continuous flow of ammonium acetate buffer. The sample is concentrated to a desired volume and dilution. After sample elution, the chelation and cleaning columns are flushed with 0.1M UP HNO_3 and 1.5M UP HNO_3 to remove any metal contamination. Both columns are conditioned with buffer-water mixture prior to next analysis.

2.6 HR-ICP-MS

ICP-MS is a high sample throughput instrument that offers ultra high sensitivity detection of elements. The main components are a nebulizer, plasma torch, interface, mass spectrometer separation and detector. Analyte atoms in solution are aspirated through a nebulizer into the spray chamber where small droplets are separated from larger droplets resulting in only 1-2 % of the sample [12]. The smaller droplets continue to become ionized by a plasma. The plasma is produced by the interaction of an electromagnetic field on a flow of gas such as argon. This results in a high temperature ($\sim$10000 K) plasma of positively charged ions. Once the analyte ions are formed they are directed by the interface region. The interface region consists of two metallic cones that guide the ions into the mass separation section. This interface region is important for the proper transfer of ions into the main vacuum chamber of the mass spectrometer. Ions then enter the ionic optic region. This region contains electrostatic lenses which keeps photons or neutral species from reaching the detector. Ions enter the mass spectrometer separation device where analyte ions are separated based on particular mass-to-charge ratio and filtering out all interfering matrix ions. High resolution ICP-MS (HR-ICP-MS) refers to a reduction of mass overlap interferences. This is achieved by a magnetic and electric sector in the mass spectrometer that separates and focuses the ions.

The magnetic sector disperses ions based on energy and mass. The electric sector disperses ions based on ion energy which allows for focusing of ions.

2.7 Chelex-100

Chelex resins are chelating agents that bind heavy metals and can be used as cleaning agents, separation or pre-concentration methods [108]. In this thesis, chelex-100 analytical grade resin [13] is used as a cleaning agent for removal of trace metal contaminants in aquil synthetic seawater and luminol reagent. Chelating resin is composed of styrene divinylbenzene copolymers containing paired iminodiacetate ions which bind polyvalent metal ions with high affinity for copper, iron and other metals. Initially, chelex resin slurry is added directly to sample where it binds with selective metals for a minimum of 1 hour. Chelex resin is then removed from sample using a filtering column. If initial metals concentration is known a resin capacity can be calculated. The wet capacity of chelex is 0.40meq/ml and density of chelex resin is 0.65g/ml. From equations 2.7- 2.9, the total grams of chelex resin needed can be calculated [13].

$$\text{Weight of metals} = \frac{\text{Total average weight of metals per volume}(mg/L)}{\text{Average equivalence}} \tag{2.7}$$

$$\text{Average equivalence} = \frac{\text{Average molecular weight of metals}}{\text{Average valence}} \tag{2.8}$$

$$\text{Chelex weight required} = \frac{\text{Weight of metals}}{\text{Chelex resin wet capacity}} \text{ Density of resin} \qquad (2.9)$$

Chapter 3

MATERIALS AND METHODS

3.1 Materials

All solutions and standards were prepared using $\geq$ 18 MΩ cm-1 deionized water. Suprapur chemicals are used for HR-ICP-MS samples, preparation of reagents for FIA-CL and final steps of acid washing. Nalgene, high density polyethylene and low density polyethylene (LDPE) are preferred material for sampling containers.

3.2 Acid washing procedure

Washing techniques for sampling equipment at trace level concentrations paved the way for accurate and precise trace elemental analysis. The following cleaning procedures for trace metal analysis comply with [27] which is based on GEOTRACES standardization initiative. The process involves a three main step system for cleaning containers, tubing and fittings.

The first step involves placing plastic in 5% detergent bath for one week followed by rinsing three times with deionized water. Then immersing the plastic in 6M reagent

grade hydrochloric acid for two weeks then rinsing three times with deionized water. The third step is immersing plastic in 3M analytical grade hydrochloric acid for two weeks then rinsing four times with ultra high purity (UHP) water.

If plastic will not be used the same day, the containers are filled with UHP water and acidified to pH ≤ 2 with UHP nitric acid until use. Once ready for use, plastic is rinsed four times with UHP water.

3.3 Aquil preparation

Aquil is a chemically defined phytoplankton culture medium for trace metal studies composed of synthetic ocean water which contains macro- and micro- nutrients. This allows for a control environment to isolate the effects of cyanobacteria culture on different trace metals. The recipe of aquil prepared is modified from [4]. The original aquil medium is proposed by [73, 83]. Modifications from the sources stated are based on the requirements observed in *Synechococcus* sp. PCC 7002 culture for the present work. The solution includes anhydrous salts, hydrous salts, major nutrients, metal stock in ethylenediaminetetraacetic acid (EDTA) and vitamin as seen on Table 3.1.

3.3.1 Synthetic ocean water and major nutrients

The first step for the preparation of aquil medium is the preparation of synthetic ocean seawater (SOW). To begin with, hydrous and anhydrous salts are dissolved separately into 6 liters of UHP water respectively then combining both types of

Table 3.1: Components of aquil medium with final molar concentrations [M].

Synthetic Ocean Water and Aquil Medium

Component	**Initial Stock [g/L dH2O]**	**Final stock [g/L dH2O]**	**Quantity Per 20 L**	**Final Molar concentration [M]**
Anhydrous salts			**[g]**	
NaCl		-	490.80	4.20E-01
Na2SO4		-	81.80	2.88E-02
KCl		-	14.00	9.39E-03
NaHCO3		-	4.00	2.38E-03
KBr		-	2.00	8.40E-04
H3BO3		-	0.06	4.85E-05
NaF		-	0.06	7.15E-05
Hydrous salts			**[g]**	
MgCl2x6H2O		-	222	5.45E-02
CaCl2x2H2O		-	30.8	1.05E-02
SrCl2x6H2O		-	0.34	6.38E-05
Major nutrients			**[mL]**	
NaH2PO4 H2O		13.8	200	1.00E-03
NaNO3		170.0	200	2.00E-02
Na2SiO3 .9H2O		28.4	20	1.00E-04
Metal/Metalloid stock			**[mL]**	
EDTA		2.920	20	1.00E-05
ZnSO4x7H2O		0.023	-	7.97E-08
MnCl2x4H2O		0.0240	-	1.21E-07
CoCl2x6H2O		0.0120	-	5.03E-08
Na2MoO4x2H2O		0.0242	-	1.00E-07
		Per 1 L [mL]		
CuSO4x5H2O	4.90	1	-	1.96E-08
Na2SeO3	1.90	1	-	1.00E-08
Vitamin			**[mL]**	
Cyanocobalamin (B12)		0.005	2	3.70E-10
Iron source			**[mL]**	
FeCl3x6H2O		0.270	1	5.00E-08
FeO(OH)		0.089	1	5.00E-08

salts into an acid washed LDPE translucent container. This is followed by the preparation of individual stock solutions of major nutrients, amounts shown in Table 3.1. Major nutrient stock concentrations are 1mM $NaH_2PO_4H_2O$, 20mM $NaNO_3$, 0.1mM $Na_2SiO_3.9H_2O$). All nutrient stocks are filter sterilized through 0.2μM filter, chelexed to remove metal contamination and stored in dark at 4°C. The aquil medium is brought up to 18L with UHP water.

3.3.2 Chelex cleaning and microwave sterilization

The pH of the aquil medium is adjusted to 6.01 to ensure the removal of iron contamination prior to chelex addition [83]. The following step is chelex cleaning aquil medium for the removal of metal impurities. 1mL chelex slurry is used per 1L aquil. Chelexed slurry is left in aquil medium for 24 hours on shaker. Chelex is then removed through filtration columns[13]. The aquil medium is then sterilized by microwave [50].

New chelex filtration columns are rinsed with UHP water and placed in 1M UHP nitric acid bath for one day then rinsed thoroughly with UHP water. Used chelex columns are filled up with 0.5M UHP nitric acid for one week and rinsed with UHP water[13]. The columns are then filled with 0.1M UHP nitric acid for five days then rinsed thoroughly with UHP water and stored in double plastic bags for future use.

3.3.3 Micronutrients and vitamin

Next is the preparation of the metal/metalloid stock solution. First intermediate stocks of copper(II) sulfate pentahydrate and sodium selenite are prepared sepa-

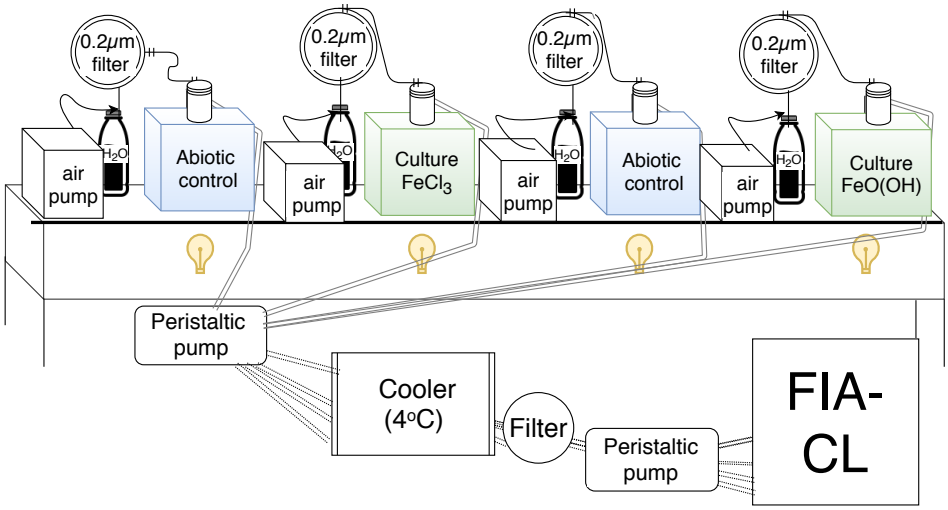

Figure 3.1: Illustration of experimental setup with abiotic and culture for FeC_3 and FeO(OH) in LDPE 20L containers.

rately as shown in Table 3.1. This is followed by the addition of 1mL copper(II) sulfate pentahydrate and sodium selenite respectively to the final metal/metalloid stock solution. The final metal/metalloid stock solution contains 2.92 g/L EDTA concentration. 20mL of the final metal/metalloid stock solution is filter sterilized and added to the aquil medium as seen in Table 3.1. Lastly, the addition of filter sterilized cyanocobalamin (vitamin B12) and iron type respectively are added to the aquil medium. The aquil medium is then brought up to 20L with UHP water.

The pH of Aquil medium is adjusted to 8.1-8.2 using UHP NH_4OH and UHP HNO_3 prior to addition of cells.

3.4 Experimental design

Starter cultures of *Synechococcus sp.* PCC 7002 wild type is taken from -80°C stocks (NTNU biotechnology group) and grown under constant illumination (75μE $m^{-2}s^{-1}$) and 38 °C in culture flasks containing 40mL modified AA+ prepared according to [123] until an OD730 of approx. 2. Cultures are washed three times by centrifuging three times at 2760g (gravitational forces) for 8 minutes followed by resuspension in iron-free aquil. For the experiments, cell to medium milliliters ratio of 1:20000 is used. Aeration for both abiotic control and cultures is supplied by bubbling filtered air through H_2O with air pumps As shown in Figure 3.1.

For the final set-up, *Synechococcus* sp. PCC 7002 is grown photoautrophically in 20 L of liquid aquil medium under constant illumination (195 μE $m^{-2}s^{-1}$) from LED lights at constant temperature (24-25 °C) [95]. A temporary trace metal free clean lab is used for the experiments. A laminar flow hood is used for sample acidification, preparation and filtration. 20 L collapsible low density polypropylene containers are used as container type. Acid washing procedures mentioned in previous sections are used for all laboratory equipment includingT teflon tubing which is used as sampling line connected to a peristaltic pump. The initial set-up for FIA-CL involves a cooler set at 4°C connected to a peristaltic pump then an inline filter (0.2μm) and enter the second peristaltic pump for FIA-CL sampling. This set up is aimed to alleviate fast oxidation during analysis of Fe(II) as a result of temperature and oxygen as discussed in theoretical section. Some complications to this set-up are discussed in later sections. As a result, manual filtration of samples is employed directly to sample vials for FIA-CL within a 30 second window for each analysis.

[a] 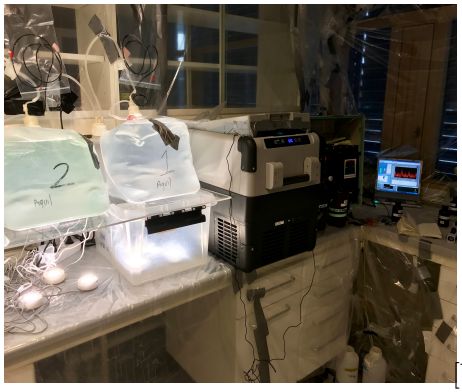 [b] 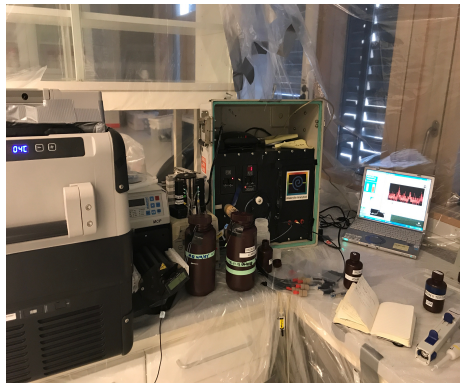

[c] 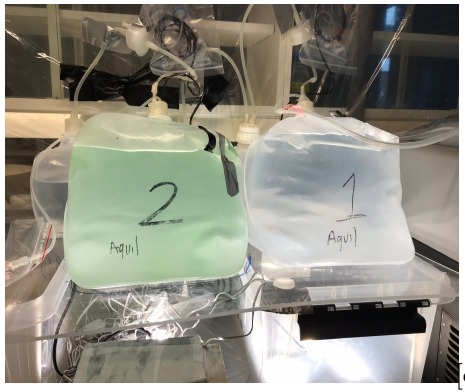 [d] 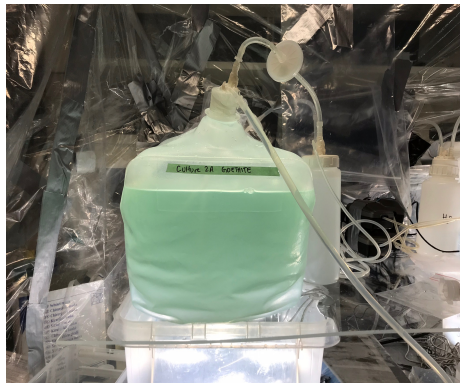

Figure 3.2: (a) Experimental set-up (b) FIA-CL set-up next to cultures with cooler and peristaltic pumps (c) *Synechococcus* sp. PCC 7002 growing with $FeCl_3$ and (d) FeO(OH) as iron source.

3.5 FIA-CL

Flow injection with luminol based chemiluminescence (FIA-CL) detection developed by FeLume Waterville Analytical, (Waterville, ME) with photomultiplier photon counter detector. Software is Labview run FIA version 2.03 with 5 samples per second and 5 sampling periods [25, 39]. Sample loop of 80cm (1mm I.D.) is used in addition to a PTFE 10-port valve (VICI Inc.). Peristaltic pump is run at 14 rpm for reagent, sample and carrier peristaltic teflon tubings. Timing parameters for loading is 40 seconds and 40 seconds for elution 1. Reagent and sample flow are 3.8 ml/min. Carrier combined flow is 8 ml/min. Ultra high purity water is used as the carrier and it is stored for 24 hours in the dark prior to analysis. Table 3.2 shows peristaltic tubing with internal diameter (I.D.) used. All sample tubing is protected from light to prevent any photochemical reactions with reagents.

Table 3.2: FIA-CL peristaltic tubing for Fe(II) analysis.

Type	Matrix	Sample tubing	I.D. [mm]	Quantity
Carrier	aged UHP water	green/green	2.06	2
Reagent	Luminol	yellow/yellow	1.42	1
Sample		green/green	2.06	1

Samples are filtered through 0.2μm pore size acid washed polycarbonate membrane filters [102]. The preparation of the luminol reagent involves 0.53g/L potassium carbonate, 0.13g/L luminol, 0.25 M ammonia solution and 11g/L UHP hydrochloric acid [40]. The final luminol pH should be between 10.0-10.2. All standards for calibrations are prepared gravimetrically and primary standard is prepared using ammonium iron (III) sulfate (50μM in 0.1 M HCl) kept for a maximum of one month. Secondary standard (50μM in 0.01M HCl) is kept for a maximum of 3 days and tertiary standard (1μM no acid) is prepared daily and used for additions

to standard in calibration curve.

3.5.1 Quality assurance

Calibrations are performed daily prior to analysis of samples. Standards for a calibration curve are made in aquil medium. Aquil medium is used as instrument blanks. Abiotic samples are used as a control to test all components in the medium without cell cultures. The limit of detection (LoD) is calculated by multiplying 3 times standard deviation of aged aquil seawater blank. A limit of detection is calculated for each calibration day and an average is reported.

$$\text{LoD}=3 \cdot \text{STDEV(blank)}$$

3.6 SeaFAST pre-concentration

The system is composed of an autosampler that is housed in a plastic cover supplied with low particulate air filter. Components are PFA Syringe modules, two 6-port valves, cleaning column, pre-concentration column and 1.0 bar pressurized Argon gas. An iminodiacetic and ethylenediaminetriacetic acid resin column is used. After concentration the samples are diluted up to 3mL with UHP water. A reference sample, NASS-7, is used to test for accuracy of seaFAST.

3.7 ICP-MS sampling

HR-ICP-MS Element 2 (Thermo Scientific) is used for the quantification of total and dissolved iron (^{56}Fe) concentration. Samples for ICP-MS are collected from tubing connected inside each culture and control container which is attached to a peristaltic pump. Sampling line is flushed through for first 20ml of sample then acid clean sampling vials are rinsed three times with sample. All samples for ICP-MS analysis are acidified with ultra pure nitric acid to pH less than 2 and stored at room temperature for at least 12 hours prior to analysis to ensure all iron is released from organic complexes and colloids [31].

3.7.1 Total Fe(III)

Total iron (TFe) samples of 6mL are collected unfiltered and acidified to 0.1M for direct analysis with ICP-MS. In addition, for ICP-MS with seaFAST 25mL sample amount is collected unfiltered and acidified (pH $\leq$ 2).

3.7.2 Dissolved iron

For direct analysis with ICP-MS, dissolved iron (dFe) samples of 6mL are filtered through a 0.2μm pore size polycarbonate membrane filter then acidified to 0.1M. In addition, for seaFAST pre-concentration method, 25mL dissolved samples (0.2μm) and acidified (pH $\leq$ 2) are collected.

Chapter 4

RESULTS

Results for FIA-CL, ICP-MS both seaFAST and direct mode in *Synechococcus* sp. PCC 7002 are shown in this section. In addition to quality assurance data such as blanks, reference material, limit of detections and calibrations. Three sample replicates are done for each sampling day for culture and control.

4.1 FIA-CL

4.1.1 Detection limits and blanks

Table 4.1 shows the limit of detection (LoD) for each calibration of the FIA-CL which is calculated based 3 times standard deviation of blank. An average of all LoD is used.

4.1.2 Calibrations

All calibrations are shown on Figure 4.1.Regression values are in appendix for each calibration. Calibrations are divided into two voltages on detector (PMT) from

Table 4.1: Limit of detection for each calibration from blanks runs.

Calibration	LoD Fe(II), (nM)
1	0.06
2	0.03
3	0.19
4	0.09
5	0.18
6	0.01
7	0.01
8	0.03
9	0.05
10	0.10
11	0.05
12	0.01
13	0.02
14	0.04
15	0.03
16	0.02
Average	**0.06**
STDEV	**0.05**
RSD %	**94.0**
LoD	**0.2 ±0.05**

Table 4.2: Blank aquil medium on FIA-CL. Each blank contains three sample replicates.

Sample	Fe(II), nM
Blank 1	0.25
Blank 2	0.38
Blank 3	0.22
Blank 4	-0.05
Blank 5	0.13
Blank 6	-0.01
Blank 7	0.31
Blank 8	0.54
Blank 9	0.21
Blank 10	0.35
Blank 11	0.22
Blank 12	0.20
Blank 13	0.19
Average	**0.23**

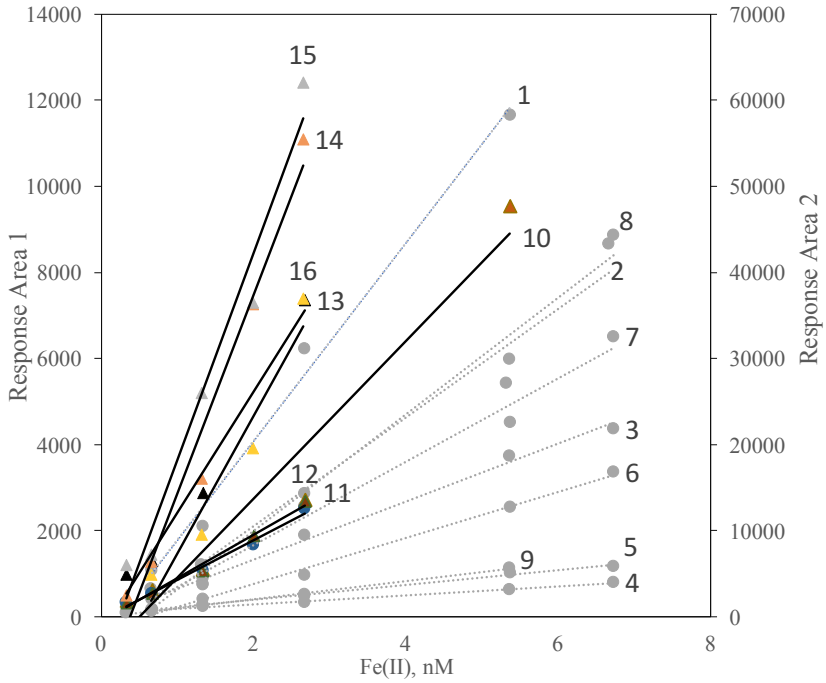

Figure 4.1: Graph represents FIA-CL calibrations for 16 total sampling times labeled (1-16). Known Fe(II) standards range between 0.33-6.7nM Fe(II) concentrations and plotted against response area. The dotted lines represent calibrations plotted on response area 1 axis and calibration lines with a solid line are plotted on response area 2 axis.

700V to 800V represented by dotted line for calibration (1-9) are on 700V voltage settings. The second set of calibrations sampling (10-16), depicted by solid lines are 900V setting. Individual calibration graphs are found in appendix.

4.1.3 Fe (II) data

First graph (Fig. 4.2a) shows culture and control with FeO(OH) and second graph (Fig. 4.2b) shows control and culture for Fe(III) chloride as the iron source. The last graph (Fig. 4.3) shows average Fe(II) concentrations for both culture experiments. All samples are corrected for blanks and LoD. Initial concentrations of iron added

are 50nM to both the control and culture which contain the same aquil medium.

For the first graph with goethite, Fe(II) is detected in culture for 6 out of 9 sampling days with the highest concentration on day 26 (0.56nM±0.01) and second highest concentrations on day 1 (0.37nM±0.01) and 8 (0.30nM±0.12). Lastly, day 11(0.12nM±0.03) and 22 (0.25nM±0.01). In control samples Fe(II) is detected for day 8 (0.34nM±0.17) and 11(0.20nM±0.20). Overall, average iron concentrations for goethite culture samples are 0.19nM±0.19 and 0.06nM±0.07 for control samples.

The second graph with $FeCl_3$ shows Fe(II) concentrations in culture for 8 out of 10 sampling days. Highest concentrations are detected on day 19 (0.69nM±0.02). Other Fe(II) detections include, day 10 (0.38nM±0.02), 15 (0.38nM±0.05), 17 (0.26nM±0.03), 21(0.37nM±0.05), 23 (0.51nM±0.01), 26 (0.19nM±0.04) and day 28 (0.20nM±0.01). In abiotic control samples Fe(II) is detected for day 15 (0.34nM±0.01) and day 28 (0.10nM±0.03). Finally, average iron concentrations for Fe(III) chloride culture samples are 0.30nM±0.22 and 0.04nM±0.22 for control samples. Complete tables can be located in appendix.

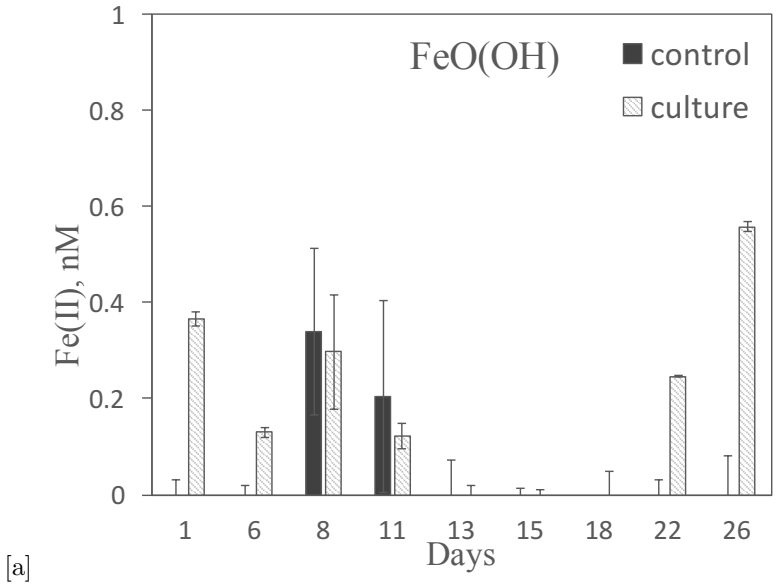

[a]

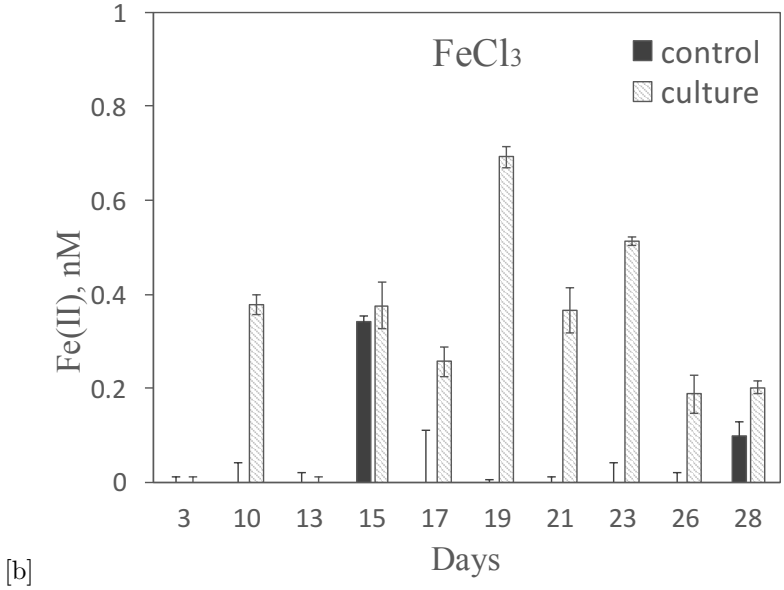

[b]

Figure 4.2: (a) Fe(II) for FeO(OH) as iron source for control and culture sample. (b) Fe(II) in culture and control containing $FeCl_3$ as iron source. Error bars represent standard deviation, n=3.

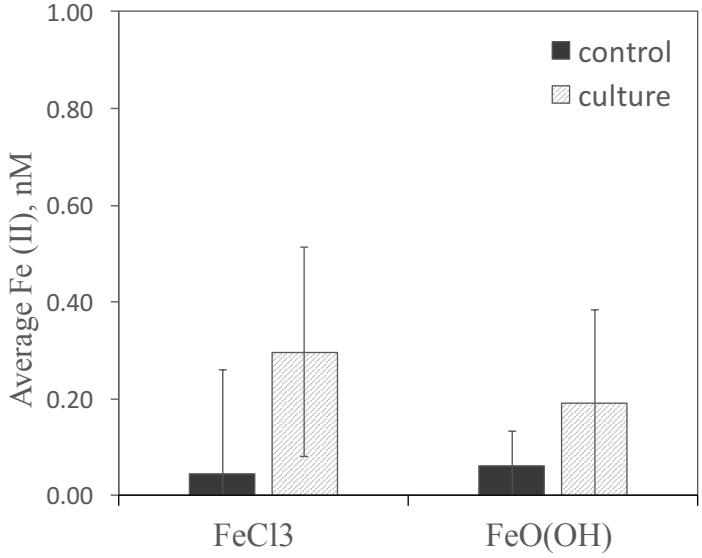

Figure 4.3: Average Fe(II) in cultures growing with $FeCl_3$ or FeO(OH). Error bars represent standard deviation, $FeCl_3$, (n=10). FeO(OH), (n=9).

4.2 ICP-MS

4.2.1 Certified reference material

Nass-7 results with seaFAST pre-concentration method with ICP-MS presented in Table 4.3 for total iron (TFe) in μg/L and corrected for concentration from seaFAST. Observed values are compared to certified reference values for accuracy.

Table 4.3: Total iron values for NASS-7 analysis on ICP-MS with seaFAST pre-concentration method. Results are corrected for blanks and concentration from seaFAST.

Sample	**TFe [μg/L]**	**Certified TFe value [μg/L]**	**Accuracy [%]**
NASS-7	0.412	0.351 ±0.9	117.5
NASS-7	0.242	0.351 ±0.9	68.8
NASS-7	0.240	0.351 ±0.9	68.4
NASS-7	0.421	0.351 ±0.9	119.8
Average	**0.329**	0.351	**93.6**

4.2.2 Detection limits and Blanks

Blanks (acidified UHP water) for seaFAST with ICP-MS samples are shown on Table 4.4. Limit of detection (0.12μgŁ) is calculated based on blank samples and standard deviation method. In addition, blanks are collected after chelex of aquil medium used for experiment and after the addition of metals (Figure 4.5).

Table 4.4: Add caption

Sample	**TFe [nM]**
Blank 1	0.03
Blank 2	1.01
Blank 3	0.87
Blank 4	0.50
Blank 5	0.58
Blank 6	0.40
Blank 7	2.21
Blank 8	1.65
Blank 9	1.45
Average	**0.97**
Stdev	**0.69**
LoD	**2.08**

Table 4.5: ICP-MS results for aquil before the addition of metals and aquil after the addition of metals with FeO(OH) and EDTA.

Sample	**TFe [nM]**
Aquil before metals	13.23
Aquil before metals	14.68
Aquil before metals	12.29
Aquil after metals	3.57
Aquil after metals	3.35
Aquil after metals	1.29

4.2.3 SeaFAST ICP-MS

Results from ICP-MS seaFAST are shown in Figures 4.5 and 4.4 . Results are converted from μg/L to nM (nmol/L).

The first set of two graphs (Fig. 4.5) shows TFe and dFe seaFAST ICP-MS results for culture and control samples with $FeCl_3$. Total and dissolved iron concentrations in culture with $FeCl_3$ samples are non-detectable with the exception of day 13 and 17 at 1.56±0.04nM and 5.84±8.21nM TFe respectively. Day 17 sample replicates are 2.31nM, 15.21nM, and nondetect. Therefore a high standard deviation for that day. Full table can be obtained in Appendix.

The next two graphs (Fig. 4.4) shows TFe and dFe seaFAST ICP-MS results for culture and control samples with FeO(OH). TFe concentrations for culture samples have average iron concentrations of 0.72±0.55nM TFe (Fig. 4.4a). Control samples show TFe concentrations below 1.5nM TFe. Dissolved iron samples shown in Figure 4.4b, are non-detectable for dissolved iron concentrations in culture except for day 15 and 22 at 1.46±0.45nM and 0.86±0.25nM respectively. For dFe in control, day 22 (1.41±0.09nM dFe) is the only day with detectable concentrations.

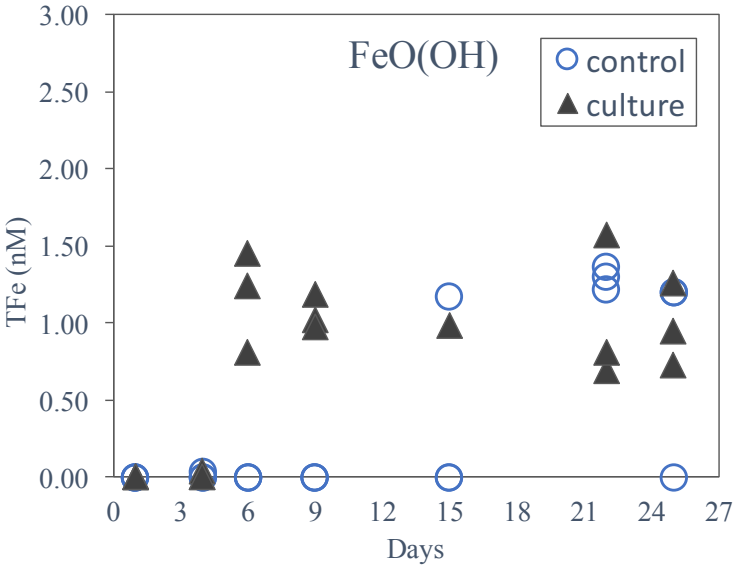

[a]

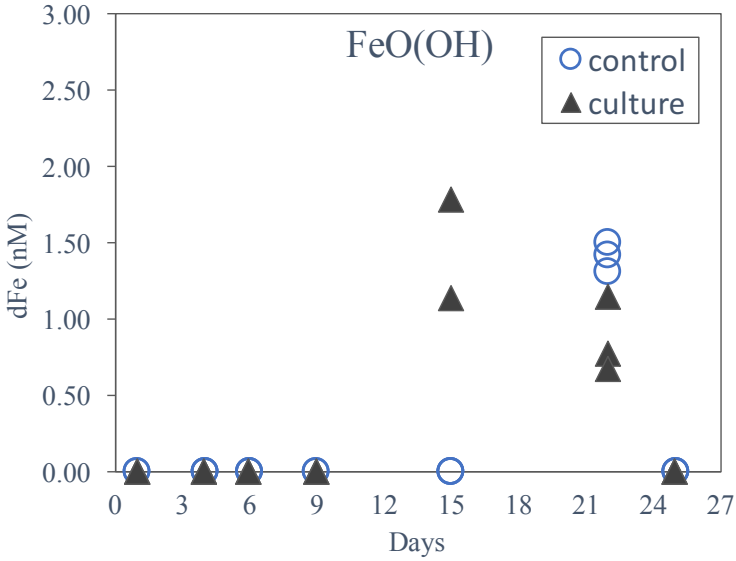

[b]

Figure 4.4: (a) Shows results for TFe and (b) for dFe using seaFAST pre-concentration method with ICP-MS for *Synechococcus* sp. PCC 7002 culture and control using FeO(OH) as iron source. Three sample replicates are collected for each control and culture sampling day as shown above.

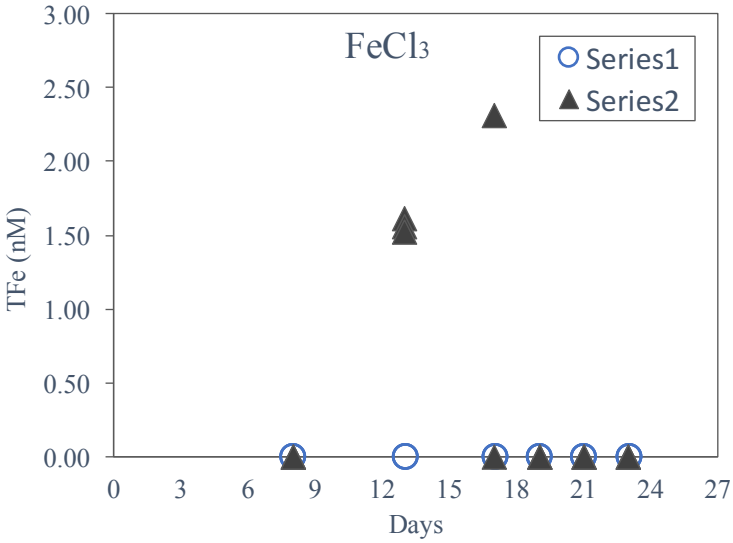

[a]

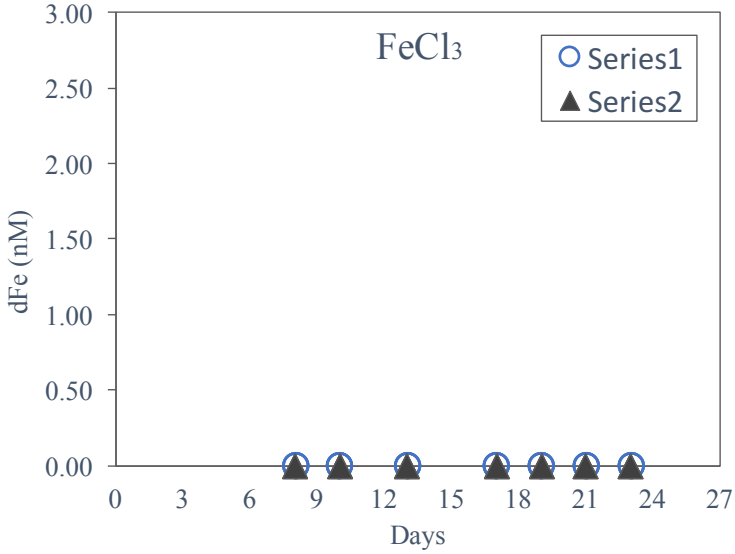

[b]

Figure 4.5: (a) Shows results for TFe and (b) for dFe using seaFAST pre-concentration method with ICP-MS for $FeCl_3$ with *Synechococcus* sp. PCC 7002 culture and control. Three sample replicates are collected for each control and culture sampling day as shown above.

4.2.4 Direct ICP-MS

Certified reference material and blanks are analyzed directly on ICP-MS (Tables 4.6 and 4.7). Blanks are composed of acidified aquil medium. Total iron results for culture with FeO(OH) are shown on Figure 4.6a. Day 1 shows 19.6±0.22nM TFe and concentration increases on day 11 to 36.5±2.85nM. Concentration on day 22 is at a relatively similar value of 37.2±1.56nM TFe from day 11. Control samples TFe results start at 13.9±1.74nM for day 1 and 17.7±0.56nM on day 11. Day 22 control samples show 19.7±0.64nM TFe. Dissolved iron results for culture with FeO(OH) shown on Figure 4.6b. Day 1 starts at 7.69±0.53nM dFe and slightly increases on day 11 to 12.0±6.04. Day 22 shows the highest concentration at 35.5±3.70nM dFe. Control samples for day 3 show 8.99±2.65nM dFe and 16.1±3.00nM dFe on day 8. Day 19 and 23 control samples show 2.67±2.71nM and 5.10±0.59nM dFe respectively.

Total iron results for culture with $FeCl_3$ shown on Figure 4.7a start at 106±1.41nM dFe for day 3 then decreases to 79.3±9.27nM on day 8, 95.3±2.57nM for day 19 and 112±4.61nM on day 23. Control samples are $21.5pm$12.06nM TFe on day 3 and 29.5±1.54nM on day 8. Additionally, control samples for day 19 and 23 show 12.2±0.79nM and 43.0±3.41nM TFe respectively. Dissolved iron results for culture with $FeCl_3$ shown on Figure 4.7b start at 14.7±9.5nM dFe for day 3 then increase to 40.5±2.2nM on day 8, 1.76±1.03nM day 19 and 3.26±1.95nM day 23. Control samples concentrations for dFe are highest on day 3 (8.99±2.65nM) and day 8 (16.1±2.96nM) then decrease on day 19 (2.67±2.72nM) and day 23(5.10±0.59nM).

Table 4.6: Certified reference material, NASS-7 is analyzed and calculated for accuracy against certified values.

Sample	**TFe [microg/L]**	**Certified TFe value [microg/L]**	**Accuracy [%]**
NASS-7	0.241	0.351	68.7
NASS-7	0.241	0.351	68.7
Average	**0.241**	0.351	**68.7**

Table 4.7: Direct ICP-MS blanks of acidified aquil.

Sample	**microg/L**	**nM**
blank	0.06	1.07
blank	0.04	0.72
blank	0.03	0.54
blank	0.07	1.25
blank	0.03	0.54
blank	0.05	0.90
blank	0.08	1.43
Average	0.05	0.92
Stdev	0.02	0.32
LoD	0.06	0.97

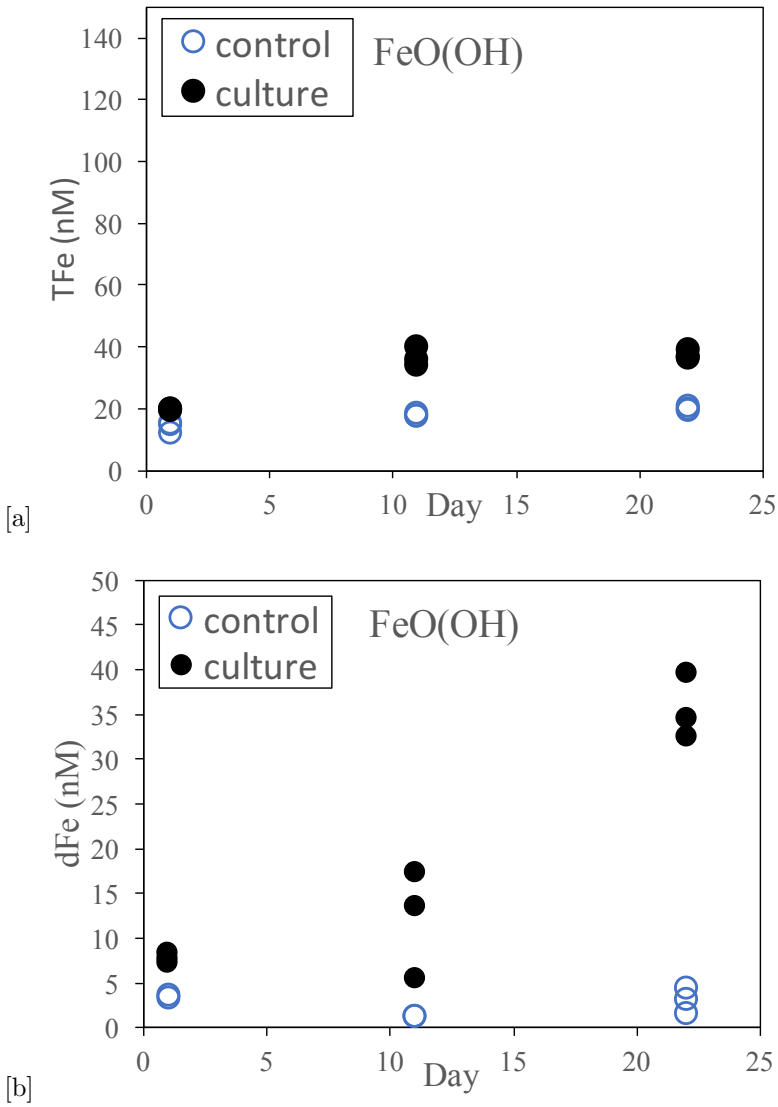

Figure 4.6: (a) Shows results for TFe and (b) for dFe for direct analysis on ICP-MS for *Synechococcus* sp. PCC 7002 culture and control using FeO(OH) as iron source. Three sample replicates are collected for each control and culture sampling day as shown above.

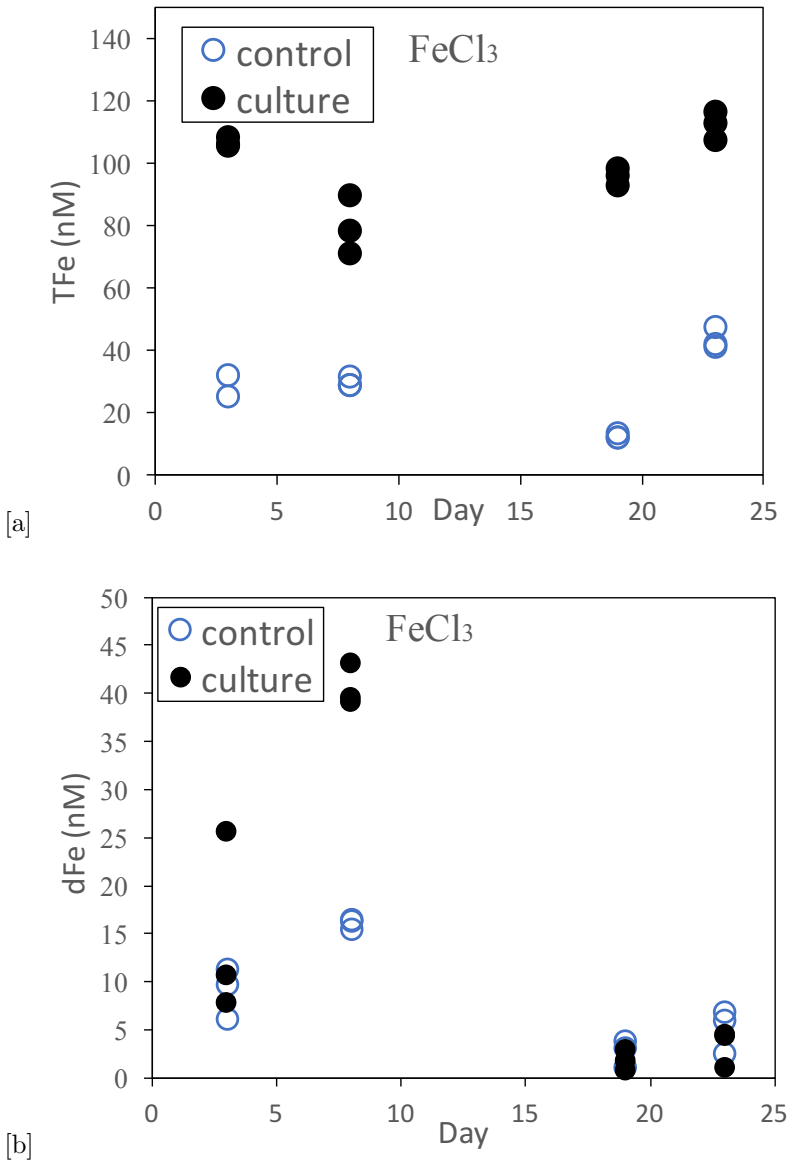

Figure 4.7: (a) Shows results for TFe and (b) for dFe for direct analysis on ICP-MS for *Synechococcus* sp. PCC 7002 culture and control using $FeCl_3$ as iron source. Three sample replicates are collected for each control and culture sampling day as shown above.

Chapter 5

DISCUSSION

The results presented aim to investigate interactions between *Synechococcus* sp. PCC 7002 and Fe(III) salts, goethite and $FeCl_3$. Changes in TFe and dFe and Fe(II) concentrations are used to determine biogenic Fe(II) production relative to abiotic control. At seawater pH, $FeCl_3$ quickly produces amorphous iron oxides ($Fe(OH)_2$) and goethite is in crystalline form [23]. The following sections will discuss FIA-CL, Fe(II), TFe and dFe results.

5.1 FIA-CL

Sample injection is an important component in FIA-CL since Fe(II) can oxidize prior to reaching the detector. As mentioned in previous sections, FIA-CL sample injection occurs through valve switching while sample line is inserted into sample container. During calibrations each calibration standard is prepared immediately before sample injection to prevent high amounts of Fe(II) oxidation. Therefore preparation of standards requires reproducible timing prior during injection to prevent any variations due to Fe(II) oxidation as a function of oxygen, pH, and temperature. This introduces some variability due to timing of sampling line injection and preparation of standards, which can be solved by the use of an autosampler.

Although autosamplers are not commonly used for FIA due to the requirement for micro level injection volumes of standard additions to achieve low detection limits. Another solution for calibrations of Fe(II) standards is the addition of acid to standards since Fe(II) is thermodynamically more stable in redox state Fe^{2+} at low pH [59], however this was not done since standards and samples should have the same matrix as required by quality assurance standards.

Additionally, uncertainties have been related to the use of peristaltic pumps since samples, reagents and carrier passes through pump tubing which controls the rate of reactions [32]. This is a larger issue for low level detections of Fe(II) such as sub-nanomolar and picomolar levels as peristaltic pump increases variability between samples which increases limits of detection. The development of piston pumps with microinjection is proposed to replace pump tubing and alleviate this uncertainty [76]. As a result, daily calibrations are required to account for systematic variations such as mentioned here. All of the calibrations in this experiment are plotted on Figure 4.1 which depict any changes in the system. A second axis is used for the last set of calibrations due to changes in the photon multiplier detector which increases sensitivity and results in larger peak areas. Additional check standards every two hours of measurement is recommended and recalibration as determined by check standard. In addition, the use of at least five calibrations standards would increase the certainty of the calibration slope.

5.2 Fe(II)

Fe(II) is an important transient specie in the ocean due to its high availability for biological uptake [61, 94, 103]. Thus Fe(II) analytical techniques allow for detail

studies in iron biochemical cycling. In the present work, Fe(II) is detected for *Synechococcus* sp. PCC 7002 with goethite (fig. 4.2a.), $FeCl_3$ (fig. 4.2b) as well as abiotic control samples (fig. 4.2). Fe(II) is detected for 6 out of 9 sampling days in goethite culture and 2 out of 9 sampling days in control samples. Despite the detection of Fe(II) in control samples, Fe(II) detection in FeO(OH) culture (0.19±0.19nM Fe(II), n=9) is three-fold higher compared to control samples (0.06±0.07nM, n=9). It should be noted the average Fe(II) concentration for goethite has a relatively high standard deviation (0.19±0.19nM) due to the gap of non-detectable Fe(II) detection for days 13, 15 and 18. This period of no Fe(II) detection may be due to several reasons. Firstly, a snapshot is obtained from FIA-CL sampling since samples are collected between 2-6 days apart depending on rate of culture growth as provided by biological measurements [82]. A continuous sampling study or increase in sampling days may reveal more information about Fe(II) concentrations in *Synechococcus* sp. PCC 7002. However, continuous FIA-CL sampling requires high volumes of luminol reagent [32, 24] which requires chelex cleaning and an increase in culture medium from 20 L is recommended.

In addition, Fe(II) is subject oxidation during manual syringe filtration. This oxidation is accounted for since all samples are prepared the same and sample timing is recorded. Filtration of samples occurs within 15 ±10 seconds of collection and it takes an additional 40 seconds for sample to reach the detector. Thus sample is exposed to oxygen which lowers the half-life of Fe(II) as seen in Figure 2.8. The oxidation of Fe(II) can be estimated based on first order kinetics and oxidant concentrations. As seen in Equation 2.3, H_2O_2 is produced from oxidation of Fe(II). Using Fig. 2.8, the half-life of Fe(II) at 25±3°C is around 20 minutes for 10nM H_2O_2 concentrations and ≤0.5 minutes for 100nM H_2O_2 concentrations and saturated O_2 levels. Fe(II) concentrations detected are expected to have oxidized

partly prior to detection. If we assume a linear relationship between half-life of iron and temperatures between 20-25°C (seen in figure 2.8) then a time zero Fe(II) estimation can be obtained [67, 97, 39]. Time zero represents the time just before the sample has been removed from the culture. For example, at 25°C, Fe(II) concentration of 0.3nM after 1 min of sampling is detected which means at time zero the concentration is 1.2nM Fe(II). In addition, if the sample analysis from the culture to the detector is 2 minutes then the time zero Fe(II) concentration is 4.8nM. Therefore it is recommended to detect for H_2O_2 concentrations in addition to be able to fully estimate Fe(II) concentration at time zero.

To reduce fast oxidation of Fe(II) during analysis, a cooler (4°C) is employed for the sampling tubing connected to 20L cultures. Sample flow goes through cooler then first peristaltic pump, followed by in-line filter (0.2μm, 60mm) and second peristaltic pump and FIA-CL. However, the flow contains many air gaps in between peristaltic pumps due to filtration which leads to inconclusive peak integrations. Particularly, increasing pump speed reduces the size of air gaps but back pressure begins to occur for pump speeds higher than 15rpm. Pump speed at 15rpm leads to difficulties in sample uptake and thereby increases Fe(II) oxidation as a function of time spent in sampling line. To improve this method it is recommended to test filters with larger volume capacities ($\geq$90mm) and tubing with larger internal diameter ($\geq$2mm) which will increase the sample flow and reduce back pressure from filtration time. A notable change in larger sample tubing is the change in sample flow which will require optimization of flow rates into FIA-CL in order to maintain sample to reagent ratio (1:1) which affects detector sensitivity. In addition, sample flow should not be high enough to introduce turbulence which will interfere with detector response [24]. To reduce oxygen effect during inline filtration, N_2 gas can be used inside the cooler. Nitrogen gas will displace oxygen

thereby reducing its oxidizing effect.

Moreover, Fe(II) detection in abiotic control samples for both goethite and Fe(III) chloride samples may be a result of photochemical reduction of iron fractions under PAR. Photochemical reduction of Fe(III) is an important component in converting Fe(III) into bioavailable forms [64, 128]. PAR reduction of FeO(OH) has still to be reported although it is shown in the presence of organic ligands such as hydrocarboxylic acid [78]. Other sources of light such as UV shows reduction of iron oxyhydroxides [52]. It is reported that UV reduction of colloidal and particulate iron can also be induced by organic compounds such as oxalate [105], citrate [125] and halogenated acetic acids [81, 56]. Organic compounds function mainly as a substrate for photoreduction [5]. Therefore, EDTA may function in facilitating Fe(III) reduction by serving as a substrate for photoreduction under PAR. In order to follow possible photochemical reduction of particulate Fe(III) an increase in Fe(II) sampling is also recommended.

Average Fe(II) concentrations in culture with $FeCl_3$ (0.30±0.22nM, n=10) are relatively higher than average Fe(II) concentrations with goethite culture (0.19±0.19nM, n=9) as shown in (Fig. 4.2b). Fe(II) is detected for culture samples with $FeCl_3$ for 8 out of 10 sampling days. Additionally, Fe(II) is detected for more days throughout the culture growth with $FeCl_3$ compared to goethite culture where Fe(II) detection is more sporadic.This is likely due to $FeCl_3$ formation of iron oxides and Fe-EDTA complexes which have higher solubility than crystalline forms (FeO(OH)) [65]. In addition, a recent study using mediated electrochemical reduction (MER) shows that thermodynamic stability of goethite strongly governs its reduction rates causing slower reduction rates compared to Ferrihydrite which is less thermodynamically stable [3]. Thus $Fe(OH)_2$ may have higher bioavailability due to its lower

thermodynamic stability which results in faster reduction rates. This is supported by average intracellular iron with $FeCl_3$ (0.39±0.08 pmolar cell^{-1} Fe) that is relatively higher than average goethite intracellular iron (0.15±0.27 pmolar cell^{-1} Fe) [82]. Thus showing that *Synechococus* sp. PCC 7002 may have more challenges in iron uptake of FeO(OH) compared to $FeCl_3$. Additionally, direct ICP-MS results show higher TFe and dFe for $FeCl_3$ (fig. 4.7) compared to goethite (fig. 4.6) which also shows higher solubility of iron forms in $FeCl_3$ compared to goethite. Although $FeCl_3$ implications are not confirmed due to probable contamination in $FeCl_3$ culture which will be discussed further in direct ICP-MS section for $FeCl_3$.

Fe(II) detected in culture relative to control may be due to cell surface iron(II) from Fe(III) reduction. This cell surface reduction occurs by extracellular protein appendages known as pili present in some bacteria [53]. Fe(II) detected may come from iron that is reduced and not rapidly absorbed by cells. It is reported that loss of Fe(II) back into the solution occurs due to the rate of reaction of Fe(II) with transporters following Fe(III) reduction at surface[55] [103]. Thus transport of Fe(II) into the cell becomes the limiting step. In an EDTA buffer medium, Fe(II) production interacts with EDTA buffer media and with membrane transporters. This may also explain low Fe(II) detection since Fe(II) is forming complexes with EDTA at faster rates than analysis.

5.3 SeaFAST with ICP-MS

TFe and dFe are determined to follow changes or transformation of Fe speciation. However, TFe and dFe results using seaFAST pre-concentration method are inconclusive with most samples below detectable limits for iron concentrations or

falling below 2.3nM (TFe and dFe) in culture and control samples. The high sample throughput of non-detect iron concentrations in not only culture samples but also control samples gives a high indication of a pre-concentration issue during seaFAST process. Interestingly, certified reference material that was analyzed together with samples have 94% Fe accuracy (see Figure 4.3). However, NASS-7 reference material does not contain EDTA. Significantly, blank samples collected to test contamination in synthetic seawater before and after metals (with EDTA addition) are shown in Figure 4.5. Aquil medium samples before metal plus EDTA addition show an average TFe concentration of 13.4±1.2nM (n=3). After the addition of metals including EDTA, TFe concentrations decrease to 2.74±1.3nM (n=3). The lower concentrations of TFe after metal addition coincide with values obtained on seaFAST for TFe concentrations (Figures 4.5 and 4.4). Blank samples support that the addition of EDTA may be involved in competing with iminodiacetic and ethylenediaminetriacetic acid (EDTA analog) resin used for pre-concentration in seaFAST. Samples are acidified to ≤pH 2 to liberate Fe from complexes, however refractory forms of iron may be present which will require lower pH for longer periods to release inorganic iron [135]. In addition UV irradiation treatment may help destroy some EDTA ligands complex with iron [52]. In the following sections of the discussion, TFe and dFe refers to direct ICP-MS sample analysis.

5.4 Direct ICP-MS

Initially, samples for direct ICP-MS analysis are collected in addition to seaFAST pre-concentration ICP-MS samples for comparison between methods. Due to low values on the majority of seaFAST results, selected samples are analyzed directly on ICP-MS for verification purposes. Results for direct ICP-MS samples are shown

in Figures 4.6 and 4.7. Figure 4.6 shows that TFe concentrations for culture growing with goethite (FeO(OH)) are initially around 20nM TFe in contrast to added amount of 50nM. This may be due to the low solubility of FeO(OH) [65] as is shown in Figure 4.6a. In particular, dFe concentrations of goethite culture (Fig. 4.6b) show an increase from sampling day 11 to 22 from 12.01±6.04nM to 35.49±3.70nM dFe. This increase in dFe concentration does not appear in control samples hence implicating a biogenic related mechanism for the increase of dFe concentration. Correspondingly, Fe(II) results for day 22 (0.17nM±0.14) (Fig. 4.2) and non-detectable Fe(II) for control can infer biological activity for the production of Fe(II). Fe(II) concentrations may have been affected by oxidation during sampling however, any Fe(II) production in culture will re-oxidize in aquil medium pH (8.00-7.36) and become part of the Fe dissolved pool. The increase in the dFe pool presented in culture can be explained by the production of Fe(II) by *Synechococcus* sp. PCC 7002 which contributes to the dFe fraction. If Fe(II) is produced, cells should also show an increase in uptake. Intracellular data for day 22 shows 41.6±9nM ^{56}Fe [82] compared to non-detectable values on days 13 and 15. However, day 11 intracellular concentration (34.7±23nM ^{56}Fe) shows higher values than particulate concentrations for the same day (30.1±16.1nM PFe) therefore likely due to introduction of iron contamination during analysis. Considering possible analytical or contamination errors for particulate and intracellular iron on day 11 still have lower iron concentrations than day 22 particulate and intracellular data. Therefore, from day 11 to day 22 of goethite culture results show an overall increase in dFe, Fe(II) and intracellular iron concentrations.

Comparatively, $FeCl_3$ results for direct ICP-MS samples are shown in Figure 4.7. TFe concentration for $FeCl_3$ culture is above the initial added concentration of 50nM $FeCl_3$ which likely represents iron obtained from contamination. One con-

tamination source comes from the incomplete chelex removal of iron shown in aquil blank samples (Fig. 4.5) which is 13.4nM±1.2 TFe. The remaining contamination may have resulted from improper capping of $FeCl_3$ culture container which led to atmosphere exposure of culture for 24 hours. Exposure of culture to atmosphere is a clear risk for contamination as discussed in introduction. Although the laboratory is in a temporary clean lab, air openings are present for the exchange of air. This contamination is also evident in average TFe particulate sample results (110nM±19, n=6) [82]. To reduce the risk of air contamination, ISO class 5 HEPA filtered systems are recommended for the air flow in laboratory [135]. For proper removal of iron contamination in aquil blanks, pre-chelex aquil blanks can be analyzed on ICP-MS for TFe to allow for proper calculations of chelex capacity volumes using Equations 2.7-2.9. In contrast, control samples for TFe (28.25±12.2nM) are below the added 50nM $FeCl_3$ concentration thus showing no signs of contamination. It is also considered that cell washing prior to inoculation as described in methods section may not have removed all iron present on cell surfaces. Although this contamination source would be present in FeO(OH) culture results. However, FeO(OH) does not show such levels of contamination observed in $FeCl_3$ cultures.

Culture with $FeCl_3$ dFe results start at 14.7±9.5nM for day 3 then increase on day 8 (40.5±2.2nM) and decreases again on day 19 (1.76±1.03nM) and day 23 (3.26±1.95nM). The increase in dFe concentration in culture with $FeCl_3$ occurring from day 3 to day 8 may indicate biogenic reduction of Fe(III) as Fe(II) is detected for day 10 (0.38±0.02nM Fe(II)) and not detected for day 3 or 13. Therefore a period of Fe(III) reduction may be occurring after formation of amorphous iron oxides or hydroxide in addition to Fe-EDTA complexes that keep Fe(III) in solution. Culture ($FeCl_3$) dFe values on day 19 (1.76±1.03nM) are much lower and indicate a decrease in Fe(III) reduction. Notably, chlorophyll-a values (chl-a)

for day 8 (1005pgChla $\cdot$ Cell^{-1}) are one order of magnitude higher than day 10 (145pgChla $\cdot$ Cell^{-1}), day 11(130pgChla $\cdot$ Cell^{-1})), day 12 (94pgChla $\cdot$ Cell^{-1})) and continue at low values until values increase again for day 22 (835pgChla $\cdot$ Cell^{-1})) [82]. Thus low chlorophyll-a values may indicate stress and collapse in cells which is also evident in a decrease of dFe concentration from day 8 sample to day 19 seen in Figure 4.7b. Average Fe(II) concentrations (Fig. 4.2) for days 10,13,15,17 (0.25$\pm$0.18nM Fe(II)) is relatively lower than days 21,23,26,28 (0.39$\pm$0.21nM Fe(II))) which coincides with the increase in chlorophyll-a values from day 22. Although Fe(II) is likely being photochemically produced in addition to biogenic reduction which explains Fe(II) detection during low chlorophyll-a values period. The control samples also show an increase in dFe concentration from day 3(9.00$\pm$2.65nM dFe) to day 8(16.1$\pm$0.59nM dFe) which shows possible photochemical reduction of Fe(III) oxides.

5.5 $FeCl_3$ and FeO(OH)

Trends for dFe in $FeCl_3$ and FeO(OH) culture show that Fe(III) reduction (biogenic and photochemical) occur sooner for $FeCl_3$ culture (between day 3-8) compared with goethite culture (between day 11-22) (Fig. 4.7a and 4.7b). This indicated that *Synechococcus* sp. PCC 7002 may be reducing amorphous salts more easily than crystalline forms. This is also indicated by average Fe(II) concentrations which are relatively higher for $FeCl_3$ (0.30$\pm$0.22nM, n=10) compared to FeO(OH) (0.19$\pm$0.19nM, n=9) culture. These differences may be due to solubilities [65] and reduction rates controlled by thermodynamic stabilities of amorphous iron oxides and crystalline iron oxyhydroxide [3]. Both abiotic control $FeCl_3$ and FeO(OH) show possibility of photochemical reduction under PAR due to Fe(II) concentra-

tions detected. It should be noted $FeCl_3$ and FeO(OH) reduction efficiencies by *Synechococcus* sp. PCC 7002 cannot be directly compared due to contamination present in $FeCl_3$ culture.

Chapter 6

CONCLUSION

Results presented in this thesis show Fe(II) detection in goethite culture in addition to an increase of dFe concentration which have implications for a reduction mechanism in *Synechococcus* sp. PCC 7002. As for $FeCl_3$ culture, Fe(II) is detected and an increase in dFe concentrations is also observed which indicate a biogenic Fe(III) reduction may also be present. Due to contamination seen in TFe of $FeCl_3$ it is difficult to compare reduction efficiencies between Fe(III) salts with crystalline forms and amorphous particles. However, dFe concentrations increase at different points in the cultures with $FeCl_3$ and FeO(OH) which may be due to thermodynamic differences between FeO(OH) and $Fe(OH)_2$ which should be studied further [3].

In addition, photochemical reduction under PAR may be a factor in abiotic reduction of Fe(III) oxyhydroxides. Higher sampling resolution is recommended to enhance methods and understanding particulate iron cycling in *Synechococcus* sp. PCC 7002 culture. These results also reveal an interference may be present for analysis using seaFAST pre-concentration method for synthetic aquil medium with EDTA. Results show that a reaction may be occurring that is stable at pH$\leq$2. Therefore higher acid concentrations are recommended in addition to UV treatment of samples prior to using seaFAST method.

Detecting iron fractions such as Fe(II) and dissolved iron is an important task for enhancing our understanding of biogeochemical cycling of iron in the ocean and its role in oceanic sequestration of atmospheric carbon dioxide. This is a growing cause as factors such as climate change continue to impact our environment which capitalizes the increasing role iron plays for primary production. However, iron determination continues to be an analytical challenge due to rapid oxidation of Fe(II) and ultra clean techniques. Despite the challenges, Fe(II) detection in *Synechococcus* sp. PCC 7002 with Fe(III) salts with varying solubilities supports possibilities for a pili reduction mechanism in *Synechococcus* sp. PCC 7002.

Chapter 7

FURTHER WORK

To further investigate the reduction of FeO(OH) by *Synechococcus* sp. PCC 7002 it is recommended to test culture with higher sampling resolution for Fe(II), TFe, DFe, PFe and intracellualr iron from day 15 to day 30. This time period observed higher Fe(II) production around day 22 and an increase in the dissolved iron pool in the same time period. It is also recommended to determine H_2O_2 concentrations in tandem with Fe(II) using FIA-CL to follow oxidant concentrations in culture. FIA-CL continuous readings will also more closely follow Fe(II) production in both cultures and control samples. In addition, Fe(II) analyses should incorporate a filtration system with cooling and possibly nitrogen purging of samples to reduce oxidation rates of Fe(II). Culture analysis is recommended without the use of EDTA to reveal information about responses to Fe(III) particles without the production of Fe-EDTA complex. In addition, photochemical reduction of amorphous iron particles and goethite should be analyzed and compared to dark and UV conditions. Iron isotope fractionation analysis ($^{54}Fe^{56}Fe^{57}Fe^{58}Fe$) is also an important tool that can be employed in *Synechococcus* sp. PCC 7002 to enable estimations of cycling of particulate iron in the culture [113, 7]. Work is also recommended to confirm the presence of pili genes in *Synechococcus* sp. PCC 7002 and additional culture studies with mutations of these genes to show their role in iron acquisition. For a deeper understanding of uptake mechanisms present in *Synechococcus* sp. PCC 7002 it is recommended to incorporate ligand analysis such as cathodic stripping

voltammetry and dissolved organic carbon (DOC) in addition to FIA-CL. These analyses will compare mechanisms for iron uptake between ligand formation and pili mediated reduction in *Synechococcus* sp. PCC 7002 under same iron conditions. Finally, variable iron types such as hermatite and Ferrihydrite will aid in increasing understanding of uptake processes of particulate iron types produced naturally in the ocean which are poorly understood.

Appendix A

ICP-MS DATA

A.1 ICP-MS with seaFAST

Table A.1: ICP-MS with seaFAST on Goethite control TFe.

SeaFAST Goethite Culture Day	Sampling date	Sample ID	Fe56(MR) UNCORRECTED		Fe56(MR) blank and dilution CORRECTED		Fe56(MR) LoD CORRECTED	
			microg/L	RSD, %	microg/L	RSD, %	microg/L	nM
1	3/20/18	G. Control. TFe. sF	0.25	7.0	0.00	7	0.00	0.00
1	3/20/18	G. Control. TFe. sF	0.19	3.7	0.00	3.7	0.00	0.00
1	3/20/18	G. Control. TFe. sF	0.23	0.8	0.00	0.8	0.00	0.00
4	3/23/18	G. Control. TFe. sF	0.37	6.3	0.00	6.3	0.00	0.03
4	3/23/18	G. Control. TFe. sF	0.25	2.3	0.00	2.3	0.00	0.00
4	3/23/18	G. Control. TFe. sF	0.23	4.7	0.00	4.7	0.00	0.00
6	3/25/18	G. Control. TFe. sF	0.25	10.0	0.00	10	0.00	0.00
6	3/25/18	G. Control. TFe. sF	0.23	5.0	0.00	5	0.00	0.00
6	3/25/18	G. Control. TFe. sF	0.20	3.2	0.00	3.2	0.00	0.00
9	3/28/18	G. Control. TFe. sF	0.61	2.3	0.04	2.3	0.00	0.00
9	3/28/18	G. Control. TFe. sF	0.60	3.7	0.04	3.7	0.00	0.00
9	3/28/18	G. Control. TFe. sF	0.58	2.9	0.03	2.9	0.00	0.00
15	4/3/18	G. Control. TFe. sF	0.63	3.7	0.04	3.7	0.00	0.00
15	4/3/18	G. Control. TFe. sF	0.58	4.6	0.03	4.6	0.00	0.00
15	4/3/18	G. Control. TFe. sF	0.80	2.2	0.07	2.2	0.07	1.17
22	4/10/18	G. Control. TFe. sF	0.87	2.1	0.08	2.1	0.08	1.36
22	4/10/18	G. Control. TFe. sF	0.81	2.0	0.07	2	0.07	1.22
22	4/10/18	G. Control. TFe. sF	0.85	4.4	0.07	4.4	0.07	1.30
25	4/13/18	G. Control. TFe. sF	0.81	2.0	0.07	2	0.07	1.20
25	4/13/18	G. Control. TFe. sF	0.81	2.5	0.07	2.5	0.07	1.20
25	4/13/18	G. Control. TFe. sF	0.51	2.9	0.02	2.9	0.00	0.00

Table A.2: ICP-MS with seaFAST on Goethite control dFe.

SeaFAST Goethite Culture Day	Sampling date	Sample ID	Fe56(MR) UNCORRECTED		Fe56(MR) blank and dilution CORRECTED		Fe56(MR) LoD CORRECTED	
			microg/L	RSD, %	microg/L	RSD, %	microg/L	nM
1	3/20/18	G.Control. dFe. sF	0.39	1.1	0.00	1.1	0.00	0.00
1	3/20/18	G.Control. dFe. sF	0.21	6.8	0.00	6.8	0.00	0.00
4	3/23/18	G.Control. dFe. sF	0.19	6.6	0.00	6.6	0.00	0.00
4	3/23/18	G.Control. dFe. sF	0.28	5.0	0.00	5	0.00	0.00
4	3/23/18	G.Control. dFe. sF	0.26	6.8	0.00	6.8	0.00	0.00
6	3/25/18	G.Control. dFe. sF	0.65	0.9	0.04	0.9	0.00	0.00
6	3/25/18	G.Control. dFe. sF	0.57	4.6	0.03	4.6	0.00	0.00
6	3/25/18	G.Control. dFe. sF	0.56	1.1	0.03	1.1	0.00	0.00
9	3/28/18	G.Control. dFe. sF	0.57	1.8	0.03	1.8	0.00	0.00
9	3/28/18	G.Control. dFe. sF	0.62	2.0	0.04	2	0.00	0.00
15	4/3/18	G.Control. dFe. sF	0.53	4.1	0.03	4.1	0.00	0.00
15	4/3/18	G.Control. dFe. sF	0.51	4.1	0.02	4.1	0.00	0.00
15	4/3/18	G.Control. dFe. sF	0.49	5.7	0.02	5.7	0.00	0.00
22	4/10/18	G.Control. dFe. sF	0.89	0.1	0.08	0.1	0.08	1.42
22	4/10/18	G.Control. dFe. sF	0.85	2.4	0.07	2.4	0.07	1.31
22	4/10/18	G.Control. dFe. sF	0.92	3.3	0.08	3.3	0.08	1.50
25	4/13/18	G.Control. dFe. sF	0.50	1.0	0.02	1	0.00	0.00
25	4/13/18	G.Control. dFe. sF	0.44	2.6	0.01	2.6	0.00	0.00
25	4/13/18	G.Control. dFe. sF	0.43	4.2	0.01	4.2	0.00	0.00

Table A.3: ICP-MS with seaFAST on Goethite culture TFe.

SeaFAST Goethite Culture Day	Sampling date	Sample ID	Fe56(MR) UNCORRECTED		Fe56(MR) blank and dilution CORRECTED		Fe56(MR) LoD CORRECTED	
			microg/L	RSD, %	microg/L	RSD, %	microg/L	nM
1	3/20/18	G.Culture.TFe.sF	0.26	1.0	0.00	1	0.00	0.00
1	3/20/18	G.Culture.TFe.sF	0.21	7.2	0.00	7.2	0.00	0.00
1	3/20/18	G.Culture.TFe.sF	0.21	6.4	0.00	6.4	0.00	0.00
4	3/23/18	G.Culture.TFe.sF	0.28	4.9	0.00	4.9	0.00	0.00
4	3/23/18	G.Culture.TFe.sF	0.37	2.3	0.00	2.3	0.00	0.04
4	3/23/18	G.Culture.TFe.sF	0.34	2.5	0.00	2.5	0.00	0.00
6	3/25/18	G.Culture.TFe.sF	0.66	1.4	0.05	1.4	0.05	0.81
6	3/25/18	G.Culture.TFe.sF	0.90	0.9	0.08	0.9	0.08	1.45
6	3/25/18	G.Culture.TFe.sF	0.82	1.6	0.07	1.6	0.07	1.24
9	3/28/18	G.Culture.TFe.sF	0.80	0.6	0.07	0.6	0.07	1.19
9	3/28/18	G.Culture.TFe.sF	0.74	5.5	0.06	5.5	0.06	1.02
9	3/28/18	G.Culture.TFe.sF	0.72	9.1	0.05	9.1	0.05	0.98
15	4/3/18	G.Culture.TFe.sF	0.73	1.4	0.06	1.4	0.06	0.99
22	4/10/18	G.Culture.TFe.sF	0.94	0.6	0.09	0.6	0.09	1.57
22	4/10/18	G.Culture.TFe.sF	0.62	3.1	0.04	3.1	0.04	0.69
22	4/10/18	G.Culture.TFe.sF	0.66	1.2	0.05	1.2	0.05	0.81
25	4/13/18	G.Culture.TFe.sF	0.63	3.1	0.04	3.1	0.04	0.73
25	4/13/18	G.Culture.TFe.sF	0.71	3.6	0.05	3.6	0.05	0.95
25	4/13/18	G.Culture.TFe.sF	0.83	3.0	0.07	3	0.07	1.26

Table A.4: ICP-MS with seaFAST on Goethite culture dFe.

SeaFAST Goethite Culture Day	Sampling date	Sample ID	Fe56(MR) UNCORRECTED		Fe56(MR) blank and dilution CORRECTED		Fe56(MR) LoD CORRECTED	
			microg/L	RSD, %	microg/L	RSD, %	microg/L	nM
1	3/20/18	G.Culture.dFe.sF	0.29	5.6	0.00	5.6	0.00	0.00
1	3/20/18	G.Culture.dFe.sF	0.18	5.0	0.00	5	0.00	0.00
1	3/20/18	G.Culture.dFe.sF	0.18	1.4	0.00	1.4	0.00	0.00
4	3/23/18	G.Culture.dFe.sF	0.20	0.5	0.00	0.5	0.00	0.00
4	3/23/18	G.Culture.dFe.sF	0.22	9.4	0.00	9.4	0.00	0.00
4	3/23/18	G.Culture.dFe.sF	0.16	0.2	0.00	0.2	0.00	0.00
6	3/25/18	G.Culture.dFe.sF	0.73	7.1	0.06	7.1	0.00	0.00
6	3/25/18	G.Culture.dFe.sF	0.63	5.9	0.04	5.9	0.00	0.00
6	3/25/18	G.Culture.dFe.sF	0.59	4.4	0.03	4.4	0.00	0.00
9	3/28/18	G.Culture.dFe.sF	0.66	7.8	0.05	7.8	0.00	0.00
9	3/28/18	G.Culture.dFe.sF	0.71	7.9	0.05	7.9	0.00	0.00
9	3/28/18	G.Culture.dFe.sF	0.69	0.7	0.05	0.7	0.00	0.00
15	4/3/18	G.Culture.dFe.sF	0.78	3.1	0.06	3.1	0.06	1.13
15	4/3/18	G.Culture.dFe.sF	1.02	3.2	0.10	3.2	0.10	1.78
22	4/10/18	G.Culture.dFe.sF	0.65	1.9	0.04	1.9	0.04	0.77
22	4/10/18	G.Culture.dFe.sF	0.79	5.5	0.06	5.5	0.06	1.15
22	4/10/18	G.Culture.dFe.sF	0.61	0.7	0.04	0.7	0.04	0.67
25	4/13/18	G.Culture.dFe.sF	0.49	5.3	0.02	5.3	0.00	0.00
25	4/13/18	G.Culture.dFe.sF	0.49	3.5	0.02	3.5	0.00	0.00
25	4/13/18	G.Culture.dFe.sF	0.55	6.4	0.03	6.4	0.00	0.00

Table A.5: ICP-MS with seaFAST on FeCl3 control TFe.

seaFAST FeCl3			Fe56(MR) UNCORRECTED		Fe56(MR) blank and dilution CORRECTED		Fe56(MR) LOD CORRECTED	
Culture Day	**Sampling date**	**Sample ID**	**microg/L**	**RSD, %**	**microg/L**	**RSD, %**	**microg/L**	**nM**
8	3/7/18	FeCl3.Control. TFe.sF	0.60	1.0	0.04	1	0.00	0.00
8	3/7/18	FeCl3.Control. TFe.sF	0.41	2.1	0.01	2.1	0.00	0.00
8	3/7/18	FeCl3.Control. TFe.sF	0.44	2.1	0.01	2.1	0.00	0.00
13	3/12/18	FeCl3.Control. TFe.sF	0.31	9.0	0.00	9	0.00	0.00
13	3/12/18	FeCl3.Control. TFe.sF	0.35	6.6	0.00	6.6	0.00	0.00
13	3/12/18	FeCl3.Control. TFe.sF	0.36	3.0	0.00	3	0.00	0.00
17	3/16/18	FeCl3.Control. TFe.sF	0.33	4.0	0.00	4	0.00	0.00
17	3/16/18	FeCl3.Control. TFe.sF	0.38	2.7	0.00	2.7	0.00	0.00
17	3/16/18	FeCl3.Control. TFe.sF	0.37	6.3	0.00	6.3	0.00	0.00
19	3/18/18	FeCl3.Control. TFe.sF	0.32	1.8	0.00	1.8	0.00	0.00
19	3/18/18	FeCl3.Control. TFe.sF	0.34	3.7	0.00	3.7	0.00	0.00
19	3/18/18	FeCl3.Control. TFe.sF	0.31	1.2	0.00	1.2	0.00	0.00
21	3/20/18	FeCl3.Control. TFe.sF	0.38	7.8	0.00	7.8	0.00	0.00
21	3/20/18	FeCl3.Control. TFe.sF	0.42	2.1	0.01	2.1	0.00	0.00
21	3/20/18	FeCl3.Control. TFe.sF	0.51	14.1	0.02	14.1	0.00	0.00
23	3/22/18	FeCl3.Control. TFe.sF	0.20	2.7	0.00	2.7	0.00	0.00
23	3/22/18	FeCl3.Control. TFe.sF	0.23	1.8	0.00	1.8	0.00	0.00
23	3/22/18	FeCl3.Control. TFe.sF	0.27	3.8	0.00	3.8	0.00	0.00

Table A.6: ICP-MS with seaFAST on FeCl3 control dFe.

seaFAST FeCl3			Fe56(MR) UNCORRECTED		Fe56(MR) blank and dilution CORRECTED		Fe56(MR) LOD CORRECTED	
Culture Day	**Sampling date**	**Sample ID**	**microg/L**	**RSD, %**	**microg/L**	**RSD, %**	**microg/L**	**nM**
8	3/7/18	FeCl3.Control.dFe.sF	0.35	2.2	0.00	2.2	0.00	0.00
8	3/7/18	FeCl3.Control.dFe.sF	0.35	2.0	0.00	2	0.00	0.00
8	3/7/18	FeCl3.Control.dFe.sF	0.35	4.3	0.00	4.3	0.00	0.00
10	3/9/18	FeCl3.Control.dFe.sF	0.32	3.6	0.00	3.6	0.00	0.00
10	3/9/18	FeCl3.Control.dFe.sF	0.33	4.7	0.00	4.7	0.00	0.00
10	3/9/18	FeCl3.Control.dFe.sF	0.53	1.2	0.03	1.2	0.00	0.00
13	3/12/18	FeCl3.Control.dFe.sF	0.36	4.9	0.00	4.9	0.00	0.00
13	3/12/18	FeCl3.Control.dFe.sF	0.30	2.8	0.00	2.8	0.00	0.00
13	3/12/18	FeCl3.Control.dFe.sF	0.43	11.8	0.01	11.8	0.00	0.00
17	3/16/18	FeCl3.Control.dFe.sF	0.29	1.5	0.00	1.5	0.00	0.00
17	3/16/18	FeCl3.Control.dFe.sF	0.58	0.8	0.03	0.8	0.00	0.00
17	3/16/18	FeCl3.Control.dFe.sF	0.32	3.7	0.00	3.7	0.00	0.00
19	3/18/18	FeCl3.Control.dFe.sF	0.29	6.2	0.00	6.2	0.00	0.00
19	3/18/18	FeCl3.Control.dFe.sF	0.36	3.3	0.00	3.3	0.00	0.00
19	3/18/18	FeCl3.Control.dFe.sF	0.32	1.8	0.00	1.8	0.00	0.00
21	3/20/18	FeCl3.Control.dFe.sF	0.31	5.4	0.00	5.4	0.00	0.00
21	3/20/18	FeCl3.Control.dFe.sF	0.23	4.7	0.00	4.7	0.00	0.00
21	3/20/18	FeCl3.Control.dFe.sF	0.18	6.2	0.00	6.2	0.00	0.00
23	3/22/18	FeCl3.Control.dFe.sF	0.20	7.6	0.00	7.6	0.00	0.00
23	3/22/18	FeCl3.Control.dFe.sF	0.21	0.4	0.00	0.4	0.00	0.00
23	3/22/18	FeCl3.Control.dFe.sF	0.19	3.4	0.00	3.4	0.00	0.00

Table A.7: ICP-MS with seaFAST on FeCl3 cultureTFe.

seaFAST FeCl3			Fe56(MR) UNCORRECTED		Fe56(MR) blank and dilution CORRECTED		Fe56(MR) LOD CORRECTED	
Culture Day	Sampling date	Sample ID	microg/L	RSD, %	microg/L	RSD, %	microg/L	nM
8	3/7/18	FeCl3.Culture. TFe.sF	0.77	2.0	0.06	2	0.00	0.00
8	3/7/18	FeCl3.Culture. TFe.sF	0.64	2.5	0.04	2.5	0.00	0.00
8	3/7/18	FeCl3.Culture. TFe.sF	0.69	5.5	0.05	5.5	0.00	0.00
13	3/12/18	FeCl3.Culture. TFe.sF	0.96	6.5	0.09	6.5	0.09	1.61
13	3/12/18	FeCl3.Culture. TFe.sF	0.94	2.0	0.09	2	0.09	1.56
13	3/12/18	FeCl3.Culture. TFe.sF	0.93	4.9	0.09	4.9	0.09	1.52
17	3/16/18	FeCl3.Culture. TFe.sF	1.22	3.5	0.13	3.5	0.13	2.31
17	3/16/18	FeCl3.Culture. TFe.sF	6.02	1.2	0.85	1.2	0.85	15.21
17	3/16/18	FeCl3.Culture. TFe.sF	0.63	4.1	0.04	4.1	0.00	0.00
19	3/18/18	FeCl3.Culture. TFe.sF	0.41	3.7	0.01	3.7	0.00	0.00
19	3/18/18	FeCl3.Culture. TFe.sF	0.37	3.5	0.00	3.5	0.00	0.00
19	3/18/18	FeCl3.Culture. TFe.sF	0.49	5.0	0.02	5	0.00	0.00
21	3/20/18	FeCl3.Culture. TFe.sF	0.33	5.0	0.00	5	0.00	0.00
21	3/20/18	FeCl3.Culture. TFe.sF	0.40	4.6	0.01	4.6	0.00	0.00
21	3/20/18	FeCl3.Culture. TFe.sF	0.52	1.8	0.02	1.8	0.00	0.00
23	3/22/18	FeCl3.Culture. TFe.sF	0.32	3.5	0.00	3.5	0.00	0.00
23	3/22/18	FeCl3.Culture. TFe.sF	0.39	1.8	0.00	1.8	0.00	0.00
23	3/22/18	FeCl3.Culture. TFe.sF	0.46	7.2	0.01	7.2	0.00	0.00

Table A.8: ICP-MS with seaFAST on FeCl3 culture dFe.

seaFAST FeCl3			Fe56(MR) UNCORRECTED		Fe56(MR) blank and dilution CORRECTED		Fe56(MR) LOD CORRECTED	
Culture Day	**Sampling date**	**Sample ID**	**microg/L**	**RSD, %**	**microg/L**	**RSD, %**	**microg/L**	**nM**
8	3/7/18	FeCl3.Culture.dFe.sF	0.43	5.1	0.01	5.1	0.00	0.00
8	3/7/18	FeCl3.Culture.dFe.sF	0.48	1.6	0.02	1.6	0.00	0.00
8	3/7/18	FeCl3.Culture.dFe.sF	0.34	6.6	0.00	6.6	0.00	0.00
10	3/9/18	FeCl3.Culture.dFe.sF	0.30	5.1	0.00	5.1	0.00	0.00
10	3/9/18	FeCl3.Culture.dFe.sF	0.28	1.4	0.00	1.4	0.00	0.00
10	3/9/18	FeCl3.Culture.dFe.sF	0.28	5.6	0.00	5.6	0.00	0.00
13	3/12/18	FeCl3.Culture.dFe.sF	0.41	1.3	0.01	1.3	0.00	0.00
13	3/12/18	FeCl3.Culture.dFe.sF	0.34	3.6	0.00	3.6	0.00	0.00
13	3/12/18	FeCl3.Culture.dFe.sF	0.30	2.4	0.00	2.4	0.00	0.00
17	3/16/18	FeCl3.Culture.dFe.sF	0.54	1.7	0.03	1.7	0.00	0.00
17	3/16/18	FeCl3.Culture.dFe.sF	0.49	4.4	0.02	4.4	0.00	0.00
17	3/16/18	FeCl3.Culture.dFe.sF	0.40	1.6	0.01	1.6	0.00	0.00
19	3/18/18	FeCl3.Culture.dFe.sF	0.35	2.7	0.00	2.7	0.00	0.00
19	3/18/18	FeCl3.Culture.dFe.sF	0.33	3.5	0.00	3.5	0.00	0.00
19	3/18/18	FeCl3.Culture.dFe.sF	0.40	4.1	0.01	4.1	0.00	0.00
21	3/20/18	FeCl3.Culture.dFe.sF	0.24	2.2	0.00	2.2	0.00	0.00
21	43179	FeCl3.Culture.dFe.sF	0.21	7.1	0.00	7.1	0.00	0.00
21	43179	FeCl3.Culture.dFe.sF	0.20	8.3	0.00	8.3	0.00	0.00
23	43181	FeCl3.Culture.dFe.sF	0.28	4.5	0.00	4.5	0.00	0.00
23	3/22/18	FeCl3.Culture.dFe.sF	0.24	6.0	0.00	6	0.00	0.00
23	3/22/18	FeCl3.Culture.dFe.sF	0.29	4.3	0.00	4.3	0.00	0.00

A.2 ICP-MS direct

Table A.9: ICP-MS direct on FeCl3 control TFe and dFe.

Direct ICPMS Culture day	Sample ID	Fe56(MR) microg/L	Fe56(MR) BLANK CORRECTED microg/L	RSD, %	Fe56(MR) nM
3	FeCl3.Control.TFe.direct	0.45	0.42	2.3	8.12
3	FeCl3.Control.TFe.direct	1.38	1.35	2.0	24.75
3	FeCl3.Control.TFe.direct	1.76	1.73	0.8	31.57
8	FeCl3.Control.TFe.direct	1.7	1.71	2.0	31.32
8	FeCl3.Control.TFe.direct	1.6	1.56	1.4	28.67
8	FeCl3.Control.TFe.direct	1.6	1.56	3.1	28.64
19	FeCl3.Control.TFe.direct	0.7	0.70	2.8	13.14
19	FeCl3.Control.TFe.direct	0.7	0.62	1.5	11.81
19	FeCl3.Control.TFe.direct	0.7	0.62	4.1	11.74
23	FeCl3.Control.TFe.direct	2.3	2.24	1.8	40.75
23	FeCl3.Control.TFe.direct	2.6	2.59	5.1	46.96
23	FeCl3.Control.TFe.direct	2.3	2.28	2.5	41.44
3	FeCl3.Control.dFe.direct	0.34	0.30	3.8	6.07
3	FeCl3.Control.dFe.direct	0.54	0.50	0.2	9.68
3	FeCl3.Control.dFe.direct	0.63	0.59	1.2	11.23
8	FeCl3.Control.dFe.direct	0.9	0.82	5.4	15.39
8	FeCl3.Control.dFe.direct	0.9	0.88	2.4	16.33
8	FeCl3.Control.dFe.direct	0.9	0.88	2.8	16.48
19	FeCl3.Control.dFe.direct	0.1	0.02	3.3	1.06
19	FeCl3.Control.dFe.direct	0.2	0.18	3.4	3.82
19	FeCl3.Control.dFe.direct	0.2	0.14	2.4	3.11
23	FeCl3.Control.dFe.direct	0.4	0.35	1.9	6.85
23	FeCl3.Control.dFe.direct	0.3	0.29	4.1	5.92
23	FeCl3.Control.dFe.direct	0.1	0.10	4.0	2.52

Table A.10: ICP-MS direct on FeCl3 culture TFe and dFe.

Direct ICPMS		**Fe56(MR)**	**Fe56(MR) BLANK COR-RECTED**		**Fe56(MR)**
Culture day	**Sample ID**	**microg/L**	**microg/L**	**RSD, %**	**nM**
3	FeCl3.Culture.TFe.direct	5.88	5.84	1.7	105.21
3	FeCl3.Culture.TFe.direct	5.89	5.85	4.2	105.49
3	FeCl3.Culture.TFe.direct	6.02	5.98	1.3	107.77
8	FeCl3.Culture.TFe.direct	4.0	3.92	1.4	70.76
8	FeCl3.Culture.TFe.direct	5.0	4.94	1.3	89.15
8	FeCl3.Culture.TFe.direct	4.4	4.32	1.0	78.01
19	FeCl3.Culture.TFe.direct	5.5	5.42	1.9	97.77
19	FeCl3.Culture.TFe.direct	5.2	5.14	0.9	92.63
19	FeCl3.Culture.TFe.direct	5.3	5.29	2.1	95.42
23	FeCl3.Culture.TFe.direct	6.3	6.25	1.6	112.50
23	FeCl3.Culture.TFe.direct	6.5	6.43	3.5	115.88
23	FeCl3.Culture.TFe.direct	6.0	5.93	2.7	106.75
3	FeCl3.Culture.dFe.direct	0.44	0.40	2.5	7.81
3	FeCl3.Culture.dFe.direct	0.59	0.56	1.7	10.62
3	FeCl3.Culture.dFe.direct	1.43	1.39	0.4	25.52
8	FeCl3.Culture.dFe.direct	2.2	2.16	0.7	39.41
8	FeCl3.Culture.dFe.direct	2.4	2.37	1.7	43.10
8	FeCl3.Culture.dFe.direct	2.2	2.15	1.6	39.07
19	FeCl3.Culture.dFe.direct	0.2	0.12	0.7	2.83
19	FeCl3.Culture.dFe.direct	0.0	0.01	10.8	0.78
19	FeCl3.Culture.dFe.direct	0.1	0.06	3.1	1.67
23	FeCl3.Culture.dFe.direct	0.2	0.21	4.1	4.44
23	FeCl3.Culture.dFe.direct	0.1	0.02	6.2	1.01
23	FeCl3.Culture.dFe.direct	0.2	0.21	2.2	4.32

Table A.11: ICP-MS direct on goethite control TFe and dFe.

Direct ICPMS Culture day	Sample ID	Fe56(MR) microg/L	Fe56(MR) BLANK CORRECTED microg/L	RSD, %	Fe56(MR) nM
1	Goethite.Control.TFe.direct	0.8	0.80	5.7	14.95
1	Goethite.Control.TFe.direct	0.8	0.79	1.0	14.78
1	Goethite.Control.TFe.direct	0.7	0.63	2.4	11.85
11	Goethite.Control.TFe.direct	1.0	0.99	6.7	18.29
11	Goethite.Control.TFe.direct	1.0	0.94	0.4	17.40
11	Goethite.Control.TFe.direct	1.0	0.93	1.3	17.26
22	Goethite.Control.TFe.direct	1.1	1.06	0.6	19.66
22	Goethite.Control.TFe.direct	1.1	1.10	2.9	20.42
22	Goethite.Control.TFe.direct	1.1	1.03	2.3	19.16
1	Goethite.Control.TFe.direct	0.2	0.16	4.7	3.58
1	Goethite.Control.dFe.direct	0.2	0.14	1.4	3.24
11	Goethite.Control.dFe.direct	0.1	0.03	2.4	1.21
11	Goethite.Control.dFe.direct	0.0	-0.06	0.2	-0.45
11	Goethite.Control.dFe.direct	0.1	0.03	3.6	1.27
22	Goethite.Control.dFe.direct	0.2	0.21	1.2	4.34
22	Goethite.Control.dFe.direct	0.1	0.05	2.2	1.55
22	Goethite.Control.dFe.direct	0.2	0.14	5.0	3.19

Table A.12: ICP-MS direct on goethite culture TFe and dFe.

Direct ICPMS		**Fe56(MR)**	**Fe56(MR) BLANK COR-RECTED**		**Fe56(MR)**
Culture day	**Sample ID**	**microg/L**	**microg/L**	**RSD, %**	**nM**
1	Goethite.Culture.TFe.direct	1.1	1.07	2.9	19.86
1	Goethite.Culture.TFe.direct	1.1	1.06	2.8	19.56
1	Goethite.Culture.TFe.direct	1.1	1.05	1.6	19.43
11	Goethite.Culture.TFe.direct	2.2	2.18	3.3	39.66
11	Goethite.Culture.TFe.direct	2.0	1.97	3.8	35.84
11	Goethite.Culture.TFe.direct	1.9	1.87	4.1	34.08
22	Goethite.Culture.TFe.direct	2.0	1.98	1.2	36.11
22	Goethite.Culture.TFe.direct	2.0	2.00	1.9	36.51
22	Goethite.Culture.TFe.direct	2.2	2.14	4.3	38.99
1	Goethite.Culture.dFe.direct	0.4	0.36	3.6	7.18
1	Goethite.Culture.dFe.direct	0.4	0.39	5.2	7.67
1	Goethite.Culture.dFe.direct	0.5	0.42	4.2	8.23
11	Goethite.Culture.dFe.direct	0.3	0.26	3.3	5.38
11	Goethite.Culture.dFe.direct	0.8	0.71	5.0	13.45
11	Goethite.Culture.dFe.direct	1.0	0.92	4.2	17.19
22	Goethite.Culture.dFe.direct	2.2	2.17	2.7	39.59
22	Goethite.Culture.dFe.direct	1.8	1.77	4.1	32.41
22	Goethite.Culture.dFe.direct	1.9	1.89	1.3	34.47

Appendix B

FIA-CL DATA

B.1 FIA-CL Calibrations

B.2 FIA-CL samples

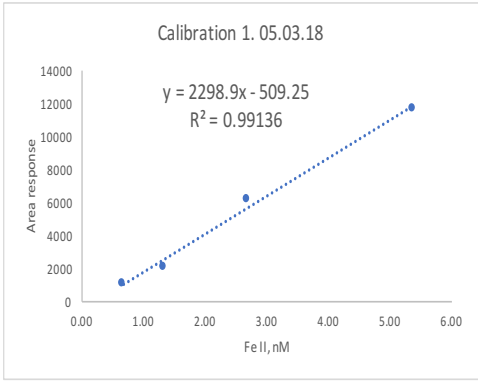
Calibration 1. 05.03.18
y = 2298.9x - 509.25
R² = 0.99136
Area response
Fe II, nM

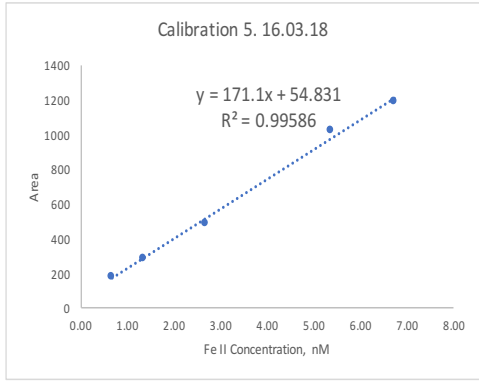
Calibration 5. 16.03.18
y = 171.1x + 54.831
R² = 0.99586
Area
Fe II Concentration, nM

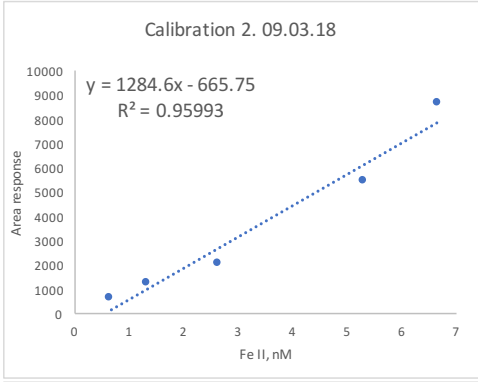
Calibration 2. 09.03.18
y = 1284.6x - 665.75
R² = 0.95993
Area response
Fe II, nM

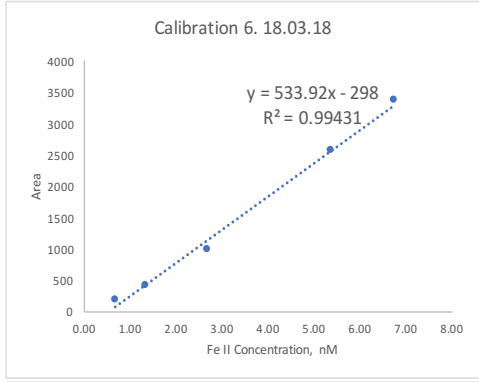
Calibration 6. 18.03.18
y = 533.92x - 298
R² = 0.99431
Area
Fe II Concentration, nM

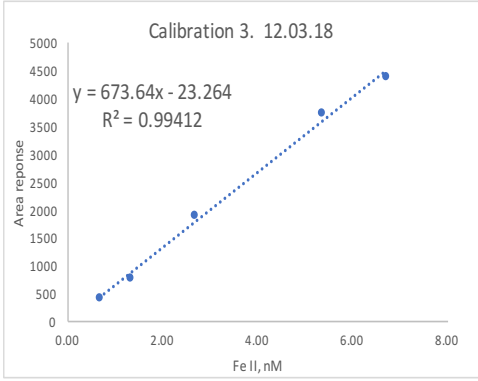
Calibration 3. 12.03.18
y = 673.64x - 23.264
R² = 0.99412
Area reponse
Fe II, nM

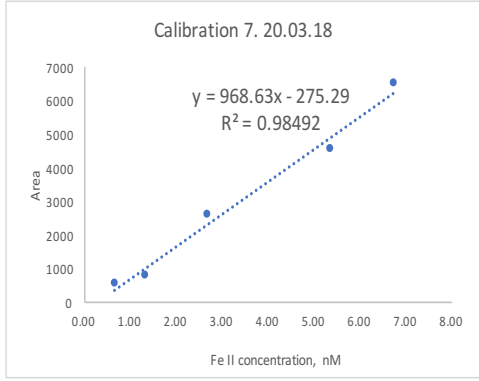
Calibration 7. 20.03.18
y = 968.63x - 275.29
R² = 0.98492
Area
Fe II concentration, nM

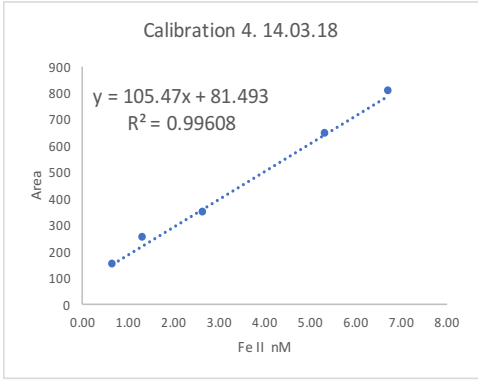
Calibration 4. 14.03.18
y = 105.47x + 81.493
R² = 0.99608
Area
Fe II nM

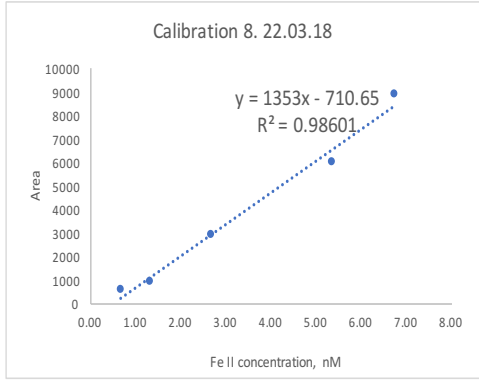
Calibration 8. 22.03.18
y = 1353x - 710.65
R² = 0.98601
Area
Fe II concentration, nM

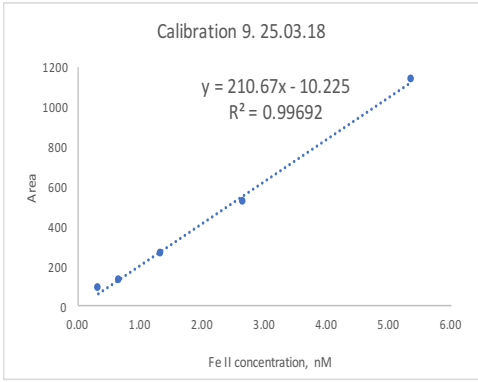
Calibration 9. 25.03.18
y = 210.67x - 10.225
R² = 0.99692
Area
Fe II concentration, nM

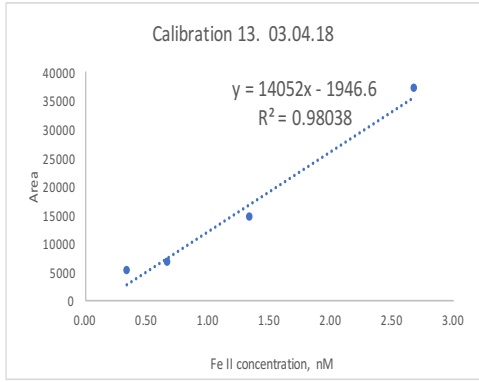
Calibration 13. 03.04.18
y = 14052x - 1946.6
R² = 0.98038
Area
Fe II concentration, nM

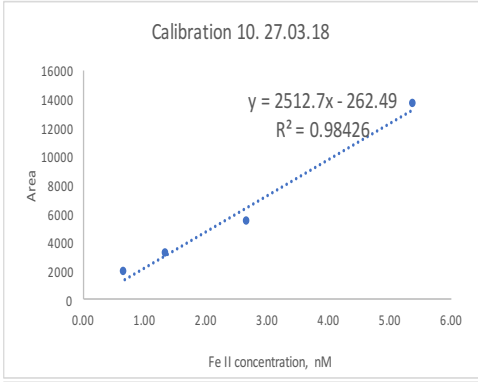
Calibration 10. 27.03.18
y = 2512.7x - 262.49
R² = 0.98426
Area
Fe II concentration, nM

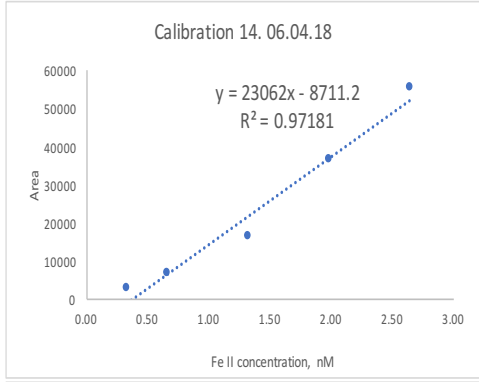
Calibration 14. 06.04.18
y = 23062x - 8711.2
R² = 0.97181
Area
Fe II concentration, nM

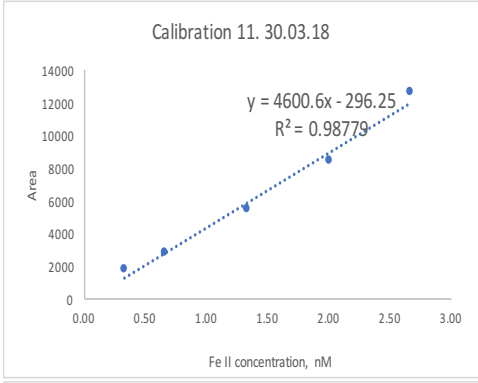
Calibration 11. 30.03.18
y = 4600.6x - 296.25
R² = 0.98779
Area
Fe II concentration, nM

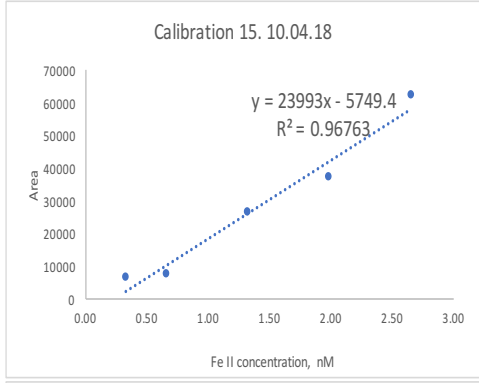
Calibration 15. 10.04.18
y = 23993x - 5749.4
R² = 0.96763
Area
Fe II concentration, nM

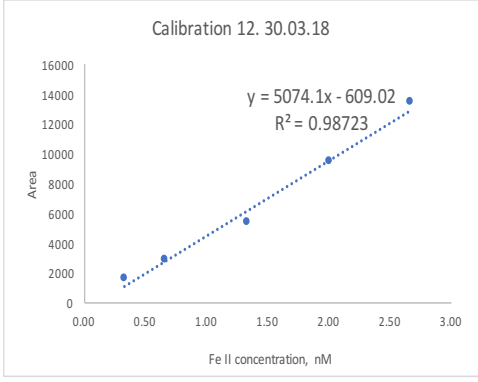
Calibration 12. 30.03.18
y = 5074.1x - 609.02
R² = 0.98723
Area
Fe II concentration, nM

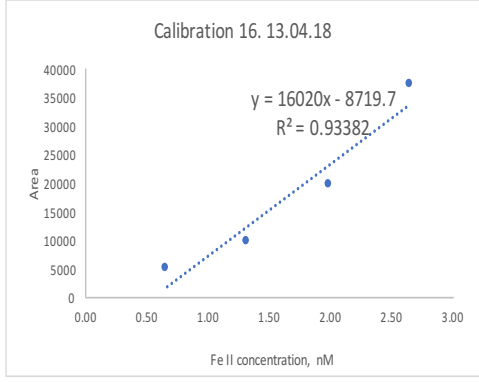
Calibration 16. 13.04.18
y = 16020x - 8719.7
R² = 0.93382
Area
Fe II concentration, nM

Table B.1: FeCl3 samples on FIA-CL

Culture day	FeCl3	Area response	Area, Blank corrected	Fe II, nM
3	**Abiotic**	0.0	0.0	0.0
		0.0	0.0	0.0
		0.0	0.0	0.0
		0.0	0.0	0.0
		0.0	0.0	0.0
		0.0	0.0	0.0
		0.0	0.0	0.0
3	**Culture**	0.0	0.0	0.0
		0.0	0.0	0.0
		0.0	0.0	0.0
		0.0	0.0	0.0
		0.0	0.0	0.0
		0.0	0.0	0.0
10	**Abiotic**	30.0	-21.0	0.0
		15.0	-36.0	0.0
		33.0	-18.0	0.0
10	**Culture**	124.0	73.0	0.4
		154.0	103.0	0.4
		109.0	58.0	0.4
		83.0	32.0	0.4
13	**Abiotic**	114.0	6.2	0.0
		104.0	-3.8	0.0
		103.0	-4.8	0.0
		100.0	-7.8	0.0
		76.0	-31.8	0.0
13	**Culture**	124.0	16.2	0.0
		114.0	6.2	0.0
		108.0	0.2	0.0
		110.0	2.2	0.0
		95.0	-12.8	0.0
		98.0	-9.8	0.0
15	**Abiotic**	108.3	33.3	0.0
		203.1	128.1	0.4
		207.0	132.0	0.5
		251.7	176.7	0.9
		214.3	139.3	0.5
15	**Culture**	190.0	115.0	0.3
		141.3	66.3	0.0
		189.5	114.5	0.3
		146.9	71.9	0.0
		116.2	41.2	0.0
		208.9	133.9	0.5
		146.2	71.2	0.0

Table B.2: FeCl3 samples on FIA-CL

Culture day	FeCl3	Area response	Area, Blank corrected	Fe II, nM
17	**Abiotic**	87.0	20.2	-0.2
		74.0	7.2	-0.3
		64.0	-2.8	-0.3
		40.0	-26.8	-0.5
		84.0	17.2	-0.2
17	**Culture**	154.0	87.2	0.2
		188.0	121.2	0.4
		130.0	63.2	0.0
		139.0	72.2	0.1
		158.0	91.2	0.2
		206.0	139.2	0.5
19	**Abiotic**	10.0	-38.5	0.0
		1.0	-47.5	0.0
		0.0	-48.5	0.0
		0.0	-48.5	0.0
19	**Culture**	140.0	91.5	0.7
		114.0	65.5	0.7
		92.0	43.5	0.6
		148.0	99.5	0.7
		118.0	69.5	0.7
		99.0	50.5	0.7
		114.0	65.5	0.7
		121.0	72.5	0.7
21	**Abiotic**	27.0	-1.4	0.0
		22.0	-6.4	0.0
		15.0	-13.4	0.0
		22.0	-6.4	0.0
		15.0	-13.4	0.0
		23.0	-5.4	0.0
21	**Culture**	166.0	137.6	0.4
		132.0	103.6	0.4
		140.0	111.6	0.4
		167.0	138.6	0.4
		100.0	71.6	0.4

Table B.3: FeCl3 samples on FIA-CL

Culture day	FeCl3	Area response	Area, Blank corrected	Fe II, nM
23	**Abiotic**	23.0	-129.0	0.0
		22.0	-130.0	0.0
		21.0	-131.0	0.0
		30.0	-122.0	0.0
		45.0	-107.0	0.0
		59.0	-93.0	0.0
		55.0	-97.0	0.0
		65.0	-87.0	0.0
23	**Culture**	158.0	6.0	0.5
		177.0	25.0	0.5
		176.0	24.0	0.5
		175.0	23.0	0.5
		155.0	3.0	0.5
		158.0	6.0	0.5
		173.1	21.1	0.5
		113.2	-38.9	0.5
26	**Abiotic**	50.0	-8.4	0.0
		56.0	-2.4	0.0
		52.0	-6.4	0.0
		55.0	-3.4	0.0
		52.9	-5.5	0.0
		55.0	-3.4	0.0
		50.0	-8.4	0.0
26	**Culture**	91.6	33.2	0.2
		93.0	34.6	0.2
		78.0	19.6	0.1
		86.0	27.6	0.2
		70.0	11.6	0.1
28	**Abiotic**	783.0	35.3	0.1
		1458.3	710.5	0.4
		747.0	-0.8	0.0
		750.0	2.3	0.0
		730.2	-17.6	0.0
28	**Culture**	1019.0	271.3	0.2
		996.8	249.0	0.2
		953.3	205.6	0.2

Table B.4: FeO(OH) samples on FIA-CL

Culture day	FeO(OH)	Area response	Area, Blank corrected	Fe II, nM
1	**Abiotic**	27.00	-1.40	0.00
		15.00	-13.40	0.00
		28.00	-0.40	0.00
		26.00	-2.40	0.00
1	**Culture**	116.00	87.60	0.28
		90.00	61.60	0.37
		100.00	71.60	0.35
		99.00	70.60	0.36
6	**Abiotic**	16.00	-42.40	0.00
		74.00	15.60	0.00
		10.00	-48.40	0.00
		16.00	-42.40	0.00
	Culture	76.00	17.60	0.13
		75.40	17.00	0.13
8	**Abiotic**	1838.30	1090.55	0.54
		1072.25	324.50	0.23
		1096.80	349.05	0.24
	Culture	1316.00	568.25	0.33
		905.00	157.25	0.17
		1606.00	858.25	0.45
		1104.47	356.72	0.25
11	**Abiotic**	3181.87	2608.87	0.63
		872.95	299.95	0.13
		910.30	337.30	0.14
		1248.30	675.30	0.21
		947.08	374.09	0.15
		1084.15	511.15	0.18
		419.68	-153.32	0.00
11	**Culture**	904.00	331.00	0.14
		904.60	331.60	0.14
		699.09	126.09	0.09
13	**Abiotic**	682.85	18.59	0.12
		681.70	17.44	0.12
		522.80	-141.46	0.00
		581.15	-83.11	0.00
13	**Culture**	475.15	-189.11	0.00
		486.50	-177.76	0.00
		467.00	-197.26	0.00

Table B.5: FeO(OH) samples on FIA-CL

Culture day	FeCl3	Area response	Area, Blank corrected	Fe II, nM
15	**Abiotic**	1001.01	313.76	0.16
		872.34	185.09	0.15
		1216.33	529.09	0.18
		540.00	-147.25	0.00
15	**Culture**	504.00	-183.25	0.00
		663.00	-24.25	0.00
		508.00	-179.25	0.00
		751.16	63.91	0.00
		621.00	-66.25	0.00
		632.00	-55.25	0.00
		526.00	-161.25	0.00
		581.00	-106.25	0.00
18	**Abiotic**	1000.00	-1045.67	0.00
		1635.00	-410.67	0.00
		2106.00	60.33	0.00
		1608.00	-437.67	0.00
		1456.00	-589.67	0.00
18	**Culture**	801.00	-1244.67	0.00
		987.00	-1058.67	0.00
		905.00	-1140.67	0.00
		800.00	-1245.67	0.00
		1141.00	-904.67	0.00
		806.00	-1239.67	0.00
22	**Abiotic**	330.00	-123.50	0.00
		236.00	-217.50	0.00
		327.00	-126.50	0.00
		292.00	-161.50	0.00
		393.00	-60.50	0.00
22	**Culture**	596.00	142.50	0.25
		560.00	106.50	0.25
		478.00	24.50	0.24
26	**Abiotic**	83.00	-256.60	0.00
		70.00	-269.60	0.00
		200.00	-139.60	0.00
26	**Culture**	450.00	110.40	0.55
		461.00	121.40	0.55
		300.00	-39.60	0.00
		743.00	403.40	0.57

BIBLIOGRAPHY

[1] Achilles, K., Church, T., Wilhelm, S., Luther, G., and Hutchins, D. (2003). Bioavailability of iron to trichodesmium colonies in the western subtropical atlantic ocean. *Limnology and Oceanography*, 48(6):2250–2255.

[2] Adly, C. L., Tremblay, J.-E., Powell, R. T., Armstrong, E., Peers, G., and Price, N. M. (2015). Response of heterotrophic bacteria in a mesoscale iron enrichment in the northeast subarctic pacific ocean.(author abstract). *Limnology & Oceanography*, 60(1).

[3] Aeppli, M., Voegelin, A., Gorski, C. A., Hofstetter, T. B., and Sander, M. (2017). Mediated electrochemical reduction of iron oxyhydroxides under defined thermodynamic boundary conditions. *Environmental science & technology*, 52(2).

[4] Andersen, R. A. (2005). *Algal culturing techniques*. Elsevier, Amsterdam, 1st edition.

[5] Barbeau, K., Rue, E. L., Trick, C. G., Bruland, K. W., and Butler, A. (2003). Photochemical reactivity of siderophores produced by marine heterotrophic bacteria and cyanobacteria based on characteristic fe(iii) binding groups. *Limnology and Oceanography*, 48(3):1069–1078.

[6] Behrenfeld and Kolber (1999). Widespread iron limitation of phytoplankton in the south pacific ocean. *Science (New York, N.Y.)*, 283(5403).

[7] Bennett, S. A., Rouxel, O., Schmidt, K., Garbe-Schönberg, D., Statham, P. J., and German, C. R. (2009). Iron isotope fractionation in a buoyant hydrothermal plume, 5 °s mid-atlantic ridge. *Geochimica et Cosmochimica Acta*, 73(19):5619–5634.

[8] Bergquist, B., Wu, J., and Boyle, E. (2007). Variability in oceanic dissolved iron is dominated by the colloidal fraction. *Geochimica et Cosmochimica Acta*, 71(12):2960–2974.

[9] Berman-Frank, I., Quigg, A., Finkel, Z. V., Irwin, A. J., and Haramaty, L. (2007). Nitrogen-fixation strategies and fe requirements in cyanobacteria. *Limnology and Oceanography*, 52(5):2260–2269.

[10] Bhaya, D., Takahashi, A., and Grossman, A. R. (2001). Light regulation of type iv pilus-dependent motility by chemosensor-like elements in synechocystis pcc6803. *Proceedings of the National Academy of Sciences of the United States of America*, 98(13):7540–7545.

[11] Bhaya, D., Watanabe, N., Ogawa, T., and Grossman, A. R. (1999). The role of an alternative sigma factor in motility and pilus formation in the cyanobacterium synechocystis sp. strain pcc6803. *Proceedings of the National Academy of Sciences of the United States of America*, 96(6).

[12] B'Hymer, C., Day, J. A., and Caruso, J. A. (2000). Evaluation of a microconcentric nebulizer and its suction effect in a capillary electrophoresis inter-

face with inductively coupled plasma mass spectrometry. *Applied Spectroscopy*, 54(7):1040–1046.

[13] Bio-Rad-Laboratories (2000). *Chelex 100 and Chelex 20 chelating ion exchange resin: Instruction manual.*

[14] Bonnain, C., Breitbart, M., and Buck, K. (2016). The ferrojan horse hypothesis: Iron-virus interactions in the ocean. *Frontiers in Marine Science*, 3.

[15] Bowie, A., Sedwick, P., and Worsfold, P. (2004). Analytical intercomparison between flow injection-chemiluminescence and flow injection-spectrophotometry for the determination of picomolar concentrations of iron in seawater. *Limnology and Oceanography: Methods*, 2(2):42–54.

[16] Boyd, P. W., Watson, A. J., Law, C. S., Abraham, E. R., Trull, T., Murdoch, R., Bakker, D. C. E., Bowie, A. R., Buesseler, K. O., Chang, H., Charette, M., Croot, P., Downing, K., Frew, R., Gall, M., Hadfield, M., Hall, J., Harvey, M., Jameson, G., Laroche, J., Liddicoat, M., Ling, R., Maldonado, M. T., Mckay, R. M., Nodder, S., Pickmere, S., Pridmore, R., Rintoul, S., Safi, K., Sutton, P., Strzepek, R., Tanneberger, K., Turner, S., Waite, A., and Zeldis, J. (2000). A mesoscale phytoplankton bloom in the polar southern ocean stimulated by iron fertilization. *Nature*, 407(6805).

[17] Boyle, E., Edmond, J., and Sholkovitz, E. (1977). The mechanism of iron removal in estuaries. *Geochimica et Cosmochimica Acta*, 41(9):1313–1324.

[18] Bristow, L. A., Mohr, W., Ahmerkamp, S., and Kuypers, M. M. (2017). Nutrients that limit growth in the ocean. *Current Biology*, 27(11):R474–R478.

[19] Bundy, R. M., Jiang, M., Carter, M., and Barbeau, K. A. (2016). Iron-binding ligands in the southern california current system: Mechanistic studies. *Frontiers in Marine Science*, 3.

[20] Byrne, R. H. and Kester, D. R. (1976). Solubility of hydrous ferric oxide and iron speciation in seawater. *Marine Chemistry*, 4(3):255–274.

[21] Cavender Bares, K. K., Mann, E. L., Chisholm, S. W., Ondrusek, M. E., and Bidigare, R. R. (1999). Differential response of equatorial pacific phytoplankton to iron fertilization. *Limnology and Oceanography*, 44(2):237–246.

[22] Chance, R., Jickells, T. D., and Baker, A. R. (2015). Atmospheric trace metal concentrations, solubility and deposition fluxes in remote marine air over the south-east atlantic. *Marine Chemistry*, 177.

[23] Cornell, R. M. (2003). *The iron oxides : structure, properties, reactions, occurences and uses*. Wiley-VCH, Weinheim, 2nd, completely rev. and extended ed. edition.

[24] Croot, P. and Laan, P. (2002). Continuous shipboard determination of fe(ii) in polar waters using flow injection analysis with chemiluminescence detection. *Analytica Chimica Acta*, 466(2):261–273.

[25] Croot, P., Laan, P., Nishioka, J., Strass, V., Cisewski, B., Boye, M., Timmermans, K., Bellerby, R., Goldson, L., Nightingale, P., and de Baar, H. (2005). Spatial and temporal distribution of fe(ii) and h2o2 during eisenex, an open ocean mescoscale iron enrichment. *Marine Chemistry*, 95(1-2):65–88.

[26] Croot, P., Streu, P., and Baker, A. (2004). Short residence time for iron in surface seawater impacted by atmospheric dry deposition from saharan dust events. *Geophysical Research Letters*, 31(23).

[27] Cutter, G. A. and Bruland, K. W. (2012). Rapid and noncontaminating sampling system for trace elements in global ocean surveys. *Limnology and Oceanography: Methods*, 10(6):425–436.

[28] Cutter, G. A., Moffett, J. W., Nielsdóttir, M. C., and Sanial, V. (2018). Multiple oxidation state trace elements in suboxic waters off peru: In situ redox processes and advective/diffusive horizontal transport. *Marine Chemistry*, 201:77–89.

[29] Ehrenreich, I. M., Waterbury, J. B., and Webb, E. A. (2005). Distribution and diversity of natural product genes in marine and freshwater cyanobacterial cultures and genomes. *Applied and Environmental Microbiology*, 71(11).

[30] Falkowski, P. and Knoll, A. (2007). *Evolution of primary producers in the sea.* Elsevier Inc.

[31] Fitzsimmons, J. N. and Boyle, E. A. (2012). An intercalibration between the geotraces goflo and the mitess/vanes sampling systems for dissolved iron concentration analyses (and a closer look at adsorption effects. *Limnology and Oceanography: Methods*, 10(6):437–450.

[32] Floor, G. H., Clough, R., Lohan, M. C., Ussher, S. J., Worsfold, P. J., and Quétel, C. R. (2015). Combined uncertainty estimation for the determination of the dissolved iron amount content in seawater using flow injection with chemilu-

minescence detection. *Limnology and Oceanography: Methods*, 13(12):673–686.

[33] Frew, R. D., Hutchins, D. A., Nodder, S., Sanudo-Wilhelmy, S., Tovar-Sanchez, A., K., L., E., H. C., and W., B. P. (2006). Particulate iron dynamics during fecycle in subantarctic waters southeast of new zealand. *Global Biogeochemical Cycles*, 20(1).

[34] Ghigo, J., Letoffe, S., and Wandersman, C. (1997). A new type of hemophore–dependent heme acquisition system of serratia marcescens reconstituted in escherichia coli. *The Journal of Bacteriology*, 179(11).

[35] Gledhill, M. and Buck, K. (2012). The organic complexation of iron in the marine environment: a review. *Frontiers In Microbiology*, 3.

[36] Gorby, Y. A., Yanina, S., Mclean, J. S., Rosso, K. M., Moyles, D., Dohnalkova, A., Beveridge, T. J., Chang, I. S., Kim, B. H., Kim, K. S., Culley, D. E., Reed, S. B., Romine, M. F., Saffarini, D. A., Hill, E. A., Shi, L., Elias, D. A., Kennedy, D. W., Pinchuk, G., Watanabe, K., Ishii, S., Logan, B., Nealson, K. H., and Fredrickson, J. K. (2006). Electrically conductive bacterial nanowires produced by shewanella oneidensis strain mr-1 and other microorganisms. *Proceedings of the National Academy of Sciences*, 103(30).

[37] Granger, J. and Price, N. M. (1999). The importance of siderophores in iron nutrition of heterotrophic marine bacteria. *Limnology and Oceanography*, 44(3):541–555.

[38] Hathorne, E. C., Haley, B., Stichel, T., Grasse, P., Zieringer, M., and Frank, M. (2012). Online preconcentration icpms analysis of rare earth elements in

seawater. *Geochemistry, Geophysics, Geosystems*, 13(1):n/a–n/a.

[39] Hopwood, M., Rapp, I., Schlosser, C., and Achterberg, E. (2017). Hydrogen peroxide in deep waters from the mediterranean sea, south atlantic and south pacific oceans. *Scientific Reports*, 7.

[40] Hopwood, M. J., Connelly, D. P., Arendt, K. E., Ejuul-Pedersen, T., Estinchcombe, M., Emeire, L., Eesposito, M., and Ekrishna, R. (2016). Seasonal changes in fe along a glaciated greenlandic fjord. *Frontiers in Earth Science*, 4.

[41] Hutchins, D., Hare, C., Weaver, R., Zhang, Y., Firme, G., DiTullio, G., Alm, M., Riseman, S., Maucher, J., Geesey, M., Trick, C., Smith, G., Rue, E., Conn, J., and Bruland, K. (2002). Phytoplankton iron limitation in the humboldt current and peru upwelling. *Limnology and Oceanography*, 47(4):997–1011.

[42] Hutchins, D., Witter, A. E., Butler, A., and Luther, G. W. I. (1999). Competition among marine phytoplankton for different chelated iron species. *Nature*.

[43] Ito, Y. and Butler, A. (2005). Structure of synechobactins, new siderophores of the marine cyanobacterium synechococcus sp. pcc 7002. *Limnology and Oceanography*, 50(6):1918–1923.

[44] Karabchevsky, A., Mosayyebi, A., and Kavokin, A. V. (2016). Tuning the chemiluminescence of a luminol flow using plasmonic nanoparticles. *Light: Science & Applications*, 5(11).

[45] Katoh, H., Hagino, N., and Ogawa, T. (2001). Iron-binding activity of futa1 subunit of an abc-type iron transporter in the cyanobacterium synechocystis sp.

strain pcc 6803. *Plant and Cell Physiology*, 42(8):823–827.

[46] Keren, N., Aurora, R., and Pakrasi, H. B. (2004). Critical roles of bacterioferritins in iron storage and proliferation of cyanobacteria. *Plant Physiology*, 135(3):1666–1673.

[47] King, D., Lin, J., and Kester, D. (1991). Spectrophotometric determination of iron(ii) in seawater at nanomolar concentrations. *Analytica Chimica Acta*, 247(1):125–132.

[48] King, D. W., Lounsbury, H. A., and Millero, F. J. (1995). Rates and mechanism of fe(ii) oxidation at nanomolar total iron concentrations. *Environmental science & technology*, 29(3).

[49] Knoll, A. H., Bambach, R. K., Payne, J. L., Pruss, S., and Fischer, W. W. (2007). Paleophysiology and end-permian mass extinction. *Earth and Planetary Science Letters*, 256(3):295–313.

[50] Kothari, V., Patadia, M., and Trivedi, N. (2011). Microwave sterilized media supports better microbial growth than autoclaved media. *Research in Biotechnology*, 2(5):63–72.

[51] Kranzler, C., Lis, H., Shaked, Y., and Keren, N. (2011). The role of reduction in iron uptake processes in a unicellular, planktonic cyanobacterium. *Environmental Microbiology*, 13(11):2990–2999.

[52] Kuma, K., Nishioka, J., and Matsunaga, K. (1996). Controls on iron(iii) hydroxide solubility in seawater; the influence of ph and natural organic chelators.

Limnology and Oceanography, 41(3):396–407.

[53] Lamb, J. J., Hill, R. E., Eaton-Rye, J. J., and Hohmann-Marriott, M. F. (2014). Functional role of pila in iron acquisition in the cyanobacterium synechocystis sp. pcc 6803. *PLOS ONE*, 9(8):1–12.

[54] Letoffe, S., Ghigo, J., and Wandersman, C. (1994). Iron acquisition from heme and hemoglobin by a serratia marcescens extracellular protein. *Proceedings of the National Academy of Sciences of the United States of America*, 91(21).

[55] Lis, H., Shaked, Y., Kranzler, C., Keren, N., and Morel, F. (2015). Iron bioavailability to phytoplankton: an empirical approach. *Isme Journal*, 9(4):1003–1013.

[56] Liu, F.-J., Huang, B.-Q., Li, S.-X., Zheng, F.-Y., and Huang, X.-G. (2016). Effect of nitrate enrichment and diatoms on the bioavailability of fe(iii) oxyhydroxide colloids in seawater. *Chemosphere*, 147(C):105–113.

[57] Liu, X. and Millero, F. J. (1999). The solubility of iron hydroxide in sodium chloride solutions. *Geochimica et Cosmochimica Acta*, 63(19-20):3487–3497.

[58] Liu, X. and Millero, F. J. (2002). The solubility of iron in seawater. *Marine Chemistry*, 77(1):43–54.

[59] Lohan, M. C., Aguilar Islas, A. M., and Bruland, K. W. (2006). Direct determination of iron in acidified (ph 1.7) seawater samples by flow injection analysis with catalytic spectrophotometric detection: Application and intercomparison. *Limnology and Oceanography: Methods*, 4(6):164–171.

[60] Ludwig, M. and Bryant, D. A. (2012). Synechococcus sp. strain pcc 7002 transcriptome: Acclimation to temperature, salinity, oxidative stress, and mixotrophic growth conditions. *Frontiers in microbiology*, 3.

[61] Maldonado, M. T., Boyd, P. W., Laroche, J., Strzepek, R., Waite, A., Bowie, A. R., Croot, P. L., Frew, R. D., and Price, N. M. (2001). Iron uptake and physiological response of phytoplankton during a mesoscale southern ocean iron enrichment. *Limnology and Oceanography*, 46(7):1802–1808.

[62] Martin, J., Gordon, R., and Fitzwater, S. (1991). The case for iron. *Limnology and Oceanography*, 36(8):1793–1802.

[63] Martin, J. H. and Fitzwater, S. E. (1988). Iron deficiency limits phytoplankton growth in the north-east pacific subarctic. *Nature*, 331(6154).

[64] Miller, W. L. and Kester, D. (1994). Photochemical iron reduction and iron bioavailability in seawater. *Journal of Marine Research*, 52(2).

[65] Millero, F. J. (1998). Solubility of fe(iii) in seawater. *Earth and Planetary Science Letters*, 154(1):323–329.

[66] Millero, F. J. and Sotolongo, S. (1989). The oxidation of fe(ii) with h2o2 in seawater. *Geochimica et Cosmochimica Acta*, 53(8):1867–1873.

[67] Millero, F. J., Sotolongo, S., and Izaguirre, M. (1987). The oxidation kinetics of fe(ii) in seawater. *Geochimica et Cosmochimica Acta*, 51(4):793–801.

[68] Millero, F. J., Yao, W., and Aicher, J. (1995). The speciation of fe(ii) and

fe(iii) in natural waters. *Marine Chemistry*, 50(1-4):21–39.

[69] Molot, L. A., Watson, S. B., Creed, I. F., Trick, C. G., Mccabe, S. K., Verschoor, M. J., Sorichetti, R. J., Powe, C., Venkiteswaran, J. J., and Schiff, S. L. (2014). A novel model for cyanobacteria bloom formation: the critical role of anoxia and ferrous iron. *Freshwater Biology*, 59(6):1323–1340.

[70] Moore, J., Doney, S. C., Glover, D. M., and Fung, I. Y. (2001). Iron cycling and nutrient-limitation patterns in surface waters of the world ocean. *Deep-Sea Research Part II*, 49(1):463–507.

[71] Morel, F. and Price, N. (1991). Limitation of productivity by trace metals in the sea. *Limnology and Oceanography*, 36(8).

[72] Morel, F. and Price, N. (2003). The biogeochemical cycles of trace metals in the oceans. *Science*, 300(5621):944–947.

[73] Morel, F., Rueter, J., Anderson, D., and Guillard, R. (1979). Aquil: a chemically defined phytoplankton culture medium for trace metal studies [toxicity, diatoms and dinoflagellates, algae]. *Journal of Phycology*, 15(2):135–141.

[74] Morel, F. M. M. (1993). *Principles and applications of aquatic chemistry*. Wiley, New York.

[75] Nielsdottir, M., Moore, C., Sanders, R., Hinz, D., and Achterberg, E. (2009). Iron limitation of the postbloom phytoplankton communities in the iceland basin. *Global Biogeochemical Cycles*, 23(3).

[76] Oliveira, H. M., Grand, M. M., Ruzicka, J., and Measures, C. I. (2015). Towards chemiluminescence detection in micro-sequential injection lab-on-valve format: A proof of concept based on the reaction between fe(ii) and luminol in seawater. *Talanta*, 133(C):107–111.

[77] O'Sullivan, D. W., Neale, P. J., Coffin, R. B., Boyd, T. J., and Osburn, C. L. (2005). Photochemical production of hydrogen peroxide and methylhydroperoxide in coastal waters. *Marine Chemistry*, 97(1-2):14–33.

[78] Öztürk, M., Croot, P. L., Bertilsson, S., Abrahamsson, K., Karlsone, B., David, R., Fransson, A., Sakshaug, E., Ozturk, M., and Karlson, B. (2004). Iron enrichment and photoreduction of iron under uv and par in the presence of hydroxycarboxylic acid: Implications for phytoplankton growth in the southern ocean. *Deep-Sea Research. Part Ii, Topical Studies In Oceanography*, 51(22-24):2841–2856.

[79] Patterson, C. (1956). Age of meteorites and the earth. *Geochimica et Cosmochimica Acta*, 10(4):230–237.

[80] Patterson, C. (1987). Global pollution measured by lead in mid-ocean sediments. *Nature*, 326(6110).

[81] Pehkonen, S. O., Siefert, R. L., and Hoffmann, M. R. (1995). Photoreduction of iron oxyhydroxides and the photooxidation of halogenated acetic acids. *Environmental science & technology*, 29(5).

[82] Pehlivan, A. (2018). Iron acquisition in cyanobacteria synechococcus sp. pcc 7002 culture. Master's thesis, NTNU.

[83] Price, N. M., Harrison, G. I., Hering, J. G., Hudson, R. J., Nirel, P. M. V., Palenik, B., and Morel, F. M. M. (1989). Preparation and chemistry of the artificial algal culture medium aquil. *Biological Oceanography*, 6(5–6):443–461.

[84] Raven, J., Evans, M., and Korb, R. (1999). The role of trace metals in photosynthetic electron transport in o2-evolving organisms. *Photosynthesis Research*, 60(2-3):111–150.

[85] Resing, J., Sedwick, P., German, C., Jenkins, W., Moffett, J., Sohst, B., and Tagliabue, A. (2015). Basin-scale transport of hydrothermal dissolved metals across the south pacific ocean. *Nature*, 523(7559):200–U140.

[86] Rijkenberg, M. J., Gerringa, L. J., Timmermans, K. R., Fischer, A. C., Kroon, K. J., Buma, A. G., Wolterbeek, B. T., and de Baar, H. J. (2008). Enhancement of the reactive iron pool by marine diatoms. *Marine Chemistry*, 109(1):29–44.

[87] Rose, A. and Waite, T. (2001). Chemiluminescence of luminol in the presence of iron(ii) and oxygen: Oxidation mechanism and implications for its analytical use. *Analytical Chemistry*, 73(24):5909–5920.

[88] Rose, A. and Waite, T. (2002). Kinetic model for fe(ii) oxidation in seawater in the absence and presence of natural organic matter. *Environmental Science & Technology*, 36(3):433–444.

[89] Rubin, M., Berman-Frank, I., and Shaked, Y. (2011). Dust- and mineral-iron utilization by the marine dinitrogen-fixer trichodesmium. *Nature Geoscience*, 4(8):529–534.

[90] Rudolf, M., Kranzler, C., Lis, H., Margulis, K., Stevanovic, M., Keren, N., and Schleiff, E. (2015). Multiple modes of iron uptake by the filamentous, siderophore-producing cyanobacterium, anabaena sp. pcc 7120. *Molecular microbiology*, 97(3).

[91] Rue, E. L. and Bruland, K. W. (1995). Complexation of iron(iii) by natural organic ligands in the central north pacific as determined by a new competitive ligand equilibration/adsorptive cathodic stripping voltammetric method. *Marine Chemistry*, 50(1):117–138.

[92] Ruzicka, J. and Hansen, E. (1975). Flow injection analyses. *Analytica Chimica Acta*, 78(1):145–157.

[93] Sahoo, S., Planavsky, N., Kendall, B., Wang, X., Shi, X., Scott, C., Anbar, A., Lyons, T., and Jiang, G. (2012). Ocean oxygenation in the wake of the marinoan glaciation. *Nature*, 489(7417):546–9.

[94] Salmon, T. P., Rose, A. L., Neilan, B. A., and Waite, T. D. (2006). The fel model of iron acquisition: Nondissociative reduction of ferric complexes in the marine environment. *Limnology and Oceanography*, 51(4):1744–1754.

[95] Samperio-Ramos, G., Santana-Casiano, J., and González-Dávila, M. (2018). Variability in the production of organic ligands, by synechococcus pcc 7002, under different iron scenarios. *Journal of Oceanography*, 74(3):277–286.

[96] Santana-Casiano, J., González-Dávila, M., and Millero, F. (2006). The role of fe(ii) species on the oxidation of fe(ii) in natural waters in the presence of o 2 and h 2o 2. *Marine Chemistry*, 99(1):70–82.

[97] Santana-Casiano, J. M., González-Dávila, M., and Millero, F. J. (2005). Oxidation of nanomolar levels of fe(ii) with oxygen in natural waters. *Environmental science & technology*, 39(7).

[98] Sarthou, G., Bucciarelli, E., Chever, F., Hansard, S., Gonzalez-Davila, M., Santana-Casiano, J., Planchon, F., and Speich, S. (2011). Labile fe(ii) concentrations in the atlantic sector of the southern ocean along a transect from the subtropical domain to the weddell sea gyre. *Biogeosciences*, 8(9):2461–2479.

[99] Schmidt, K., Schlosser, C., Atkinson, A., Fielding, S., Venables, H. j., Waluda, C. m., and Achterberg, E. p. (2016). Zooplankton gut passage mobilizes lithogenic iron for ocean productivity. *Current Biology*, 26(19):2667–2673.

[100] Schrader, P. S., Milligan, A. J., and Behrenfeld, M. J. (2011). Surplus photosynthetic antennae complexes underlie diagnostics of iron limitation in a cyanobacterium (excess photosynthetic antennae and iron limitation). *PLoS ONE*, 6(4).

[101] Scott, C., Lyons, T., Bekker, A., Shen, Y., Poulton, S., Chu, X., and Anbar, A. (2008). Tracing the stepwise oxygenation of the proterozoic ocean. *Nature*, 452(7186):456–459.

[102] Sedwick, P., Bowie, A., and Trull, T. (2008). Dissolved iron in the australian sector of the southern ocean (clivar sr3 section): Meridional and seasonal trends. *Deep-Sea Research Part I*, 55(8):911–925.

[103] Shaked, Y., Kustka, A., and Morel, F. (2005). A general kinetic model for iron acquisition by eukaryotic phytoplankton. *Limnology and Oceanography*,

50(3):872–882.

[104] Siddiqui, M., AlOthman, Z., and Rahman, N. (2017). Analytical techniques in pharmaceutical analysis: A review. *Arabian Journal of Chemistry*, 10:S1409–S1421.

[105] Siffert, C. and Sulzberger, B. (1991). Light-induced dissolution of hematite in the presence of oxalate - a case study. *Langmuir*, 7(8):1627–1634.

[106] Simon, N., Cras, A.-L., Foulon, E., and Lemée, R. (2009). Diversity and evolution of marine phytoplankton. *Comptes Rendus Biologies*, 332(2-3):159–170.

[107] Sohrin, Y., Urushihara, S., Nakatsuka, S., Kono, T., Higo, E., Minami, T., Norisuye, K., and Umetani, S. (2008). Multielemental determination of geotraces key trace metals in seawater by icpms after preconcentration using an ethylenediaminetriacetic acid chelating resin. *Analytical chemistry*, 80(16).

[108] Søndergaard, J., Asmund, G., and Larsen, M. (2015). Trace elements determination in seawater by icp-ms with on-line pre-concentration on a chelex-100 column using a 'standard' instrument setup. *MethodsX*, 2:323–330.

[109] Stallard, R. F. and Edmond, J. M. (1983). Geochemistry of the amazon; 2, the influence of geology and weathering environment on the dissolved load. *Journal of Geophysical Research*, 88(14):9671–9688.

[110] Statham, P. J., Jacobson, Y., and van Den Berg, C. (2012). The measurement of organically complexed feii in natural waters using competitive ligand reverse

titration. *Analytica Chimica Acta*, 743:111–116.

[111] Steele, J. H. and Henderson, E. W. (1992). The role of predation in plankton models. *Journal of Plankton Research*, 14(1):157–172.

[112] Sunda, W. G. and Huntsman, S. A. (1994). Photoreduction of manganese oxides in seawater. *Marine Chemistry*, 46(1):133–152.

[113] Swanner, E. D., Bayer, T., Wu, W., Hao, L., Obst, M., Sundman, A., Byrne, J. M., Michel, F. M., Kleinhanns, I. C., Kappler, A., and Schoenberg, R. (2017). Iron isotope fractionation during fe(ii) oxidation mediated by the oxygen-producing marine cyanobacterium synechococcus pcc 7002. *Environmental science & technology*, 51(9).

[114] Tagliabue, A., Aumont, O., and Bopp, L. (2014a). The impact of different external sources of iron on the global carbon cycle. *Geophysical Research Letters*, 41(3):920–926.

[115] Tagliabue, A., Bowie, A. R., Boyd, P. W., Buck, K. N., Johnson, K. S., and Saito, M. A. (2017). The integral role of iron in ocean biogeochemistry. *Nature*, 543(7643).

[116] Tagliabue, A., Mtshali, T., Aumont, O., Bowie, A., Klunder, M., Roychoudhury, A., and Swart, S. (2012). A global compilation of dissolved iron measurements: focus on distributions and processes in the southern ocean. *Biogeosciences*, 9(6).

[117] Tagliabue, A., Sallee, J.-B., Bowie, A. R., Levy, M., Swart, S., and Boyd,

P. W. (2014b). Surface-water iron supplies in the southern ocean sustained by deep winter mixing. *Nature Geoscience*, 7(4):314–320.

[118] Tortell, P., Maldonado, M., and Price, N. (1996). The role of heterotrophic bacteria in iron-limited ocean ecosystems. *Nature*, 383(6598):330–332.

[119] Turner, D. R. and Hunter, K. A. (2001). *The Biogeochemistry of iron in seawater*, volume vol. 7 of *IUPAC series on analytical and physical chemistry of environmental systems*. Wiley, Chichester.

[120] Twining, B. S. and Baines, S. B. (2013). The trace metal composition of marine phytoplankton. *Annual Review of Marine Science*, 5(1):191–215. PMID: 22809181.

[121] Uitz, J., Claustre, H., Gentili, B., and Stramski, D. (2010). Phytoplankton classspecific primary production in the world's oceans: Seasonal and interannual variability from satellite observations. *Global Biogeochemical Cycles*, 24(3):n/a–n/a.

[122] Ussher, S. J., Achterberg, E. P., Powell, C., Baker, A. R., Jickells, T. D., Torres, R., and Worsfold, P. J. (2013). Impact of atmospheric deposition on the contrasting iron biogeochemistry of the north and south atlantic ocean. *Global Biogeochemical Cycles*, 27(4):1096–1107. ©2013. American Geophysical Union. All Rights Reserved. Funded by: NERC. Grant Number: NER/A/S/2003/00489 and AMT Consortium. Grant Numbers: NER/O/S2001/00680, NE/c001737/1.

[123] Vogel, A. I. M., Lale, R., and Hohmann-Marriott, M. F. (2017). Streamlining recombination-mediated genetic engineering by validating three neutral

integration sites in sp. pcc 7002. *Journal of biological engineering*, 11.

[124] Von der Heyden, B. and Roychoudhury, A. (2015). A review of colloidal iron partitioning and distribution in the open ocean. *Marine Chemistry*, 177.

[125] Waite, T. and Morel, F. M. (1984). Photoreductive dissolution of colloidal iron oxide: Effect of citrate. *Journal of Colloid And Interface Science*, 102(1):121–137.

[126] Wang, W. and Dei, R. (2003). Bioavailability of iron complexed with organic colloids to the cyanobacteria synechococcus and trichodesmium. *Aquatic Microbial Ecology*, 33(3):247–259.

[127] Wang, X., Cardwell, T., Cattrall, R., Dyson, R., and Jenkins, G. (1998). Time-division multiplex technique for producing concentration profiles in flow analysis. *Analytica Chimica Acta*, 368(1-2):105–111.

[128] Wells, M. L., Mayer, L. M., Donard, O. F. X., Sierra, M. M. D. S., and Ackelson, S. G. (1991). The photolysis of colloidal iron in the oceans. *Nature*, 353(6341).

[129] Wells, M. L., Price, N. M., and Bruland, K. W. (1995). Iron chemistry in seawater and its relationship to phytoplankton: a workshop report. *Marine Chemistry*, 48(2):157–182.

[130] Wilhelm, S., Maxwell, D., and Trick, C. (1996). Growth, iron requirements, and siderophore production in iron-limited synechococcus pcc 72. *Limnology and Oceanography*, 41(1):89–97.

[131] Wilhelm, S. and Trick, C. (1994). Iron-limited growth of cyanobacteria: Multiple siderophore production is a common response. *Limnology and Oceanography*, 39(8):1979–1984.

[132] Worsfold, P. J., Clough, R., Lohan, M. C., Monbet, P., Ellis, P. S., Quétel, C. R., Floor, G. H., and Mckelvie, I. D. (2013). Flow injection analysis as a tool for enhancing oceanographic nutrient measurements—a review. *Analytica Chimica Acta*, 803:15–40.

[133] Worsfold, P. J., Lohan, M. C., Ussher, S. J., and Bowie, A. R. (2014). Determination of dissolved iron in seawater: A historical review. *Marine Chemistry*, 166:25–35.

[134] Wu, J., Boyle, E., Sunda, W., and Wen, L.-S. (2001). Soluble and colloidal iron in the oligotrophic north atlantic and north pacific. *Science*, 293(5531):847–849.

[135] Wurl, O. (2009). *Practical Guidelines for the Analysis of Seawater*. CRC press.

[136] Yeats, P., Bewers, J., and Walton, A. (1978). Sensitivity of coastal waters to anthropogenic trace metal emissions. *Marine Pollution Bulletin*, 9(10):264–268.

[137] Yi, Z., Zhuang, G., Brown, P., and Duce, R. (1992). High-performance liquid chromatographic method for the determination of ultratrace amounts of iron(ii) in aerosols, rainwater, and seawater. *Analytical Chemistry*, 64(22).